ABSTRACT

MOTAIB, SAFIYYAH ABDELHAK. Investigating the Mechanisms of Action of Metformin at Pharmacological Dose (Under the direction of Dr. Xiaojing Liu)

Metformin has been the first line treatment for type-2 diabetes globally for the past fifty years; however, its mechanisms of action are very much unclear. Hundreds of studies have been conducted attempting to understand the drug's hypoglycemic properties, alleged anti-aging properties, and potential anti-cancerous properties. Despite a vast amount of literature, metformin's mechanisms remain elusive.

It is likely whatever pathways metformin works through, it does so in a weak and transient manner, and highly depends on the type of tissue it is in as well as nutrient availability. Unfortunately, many studies use supra-pharmacological doses of metformin, therefore masking the drug's actual mechanisms. Epidemiological studies in patients taking metformin for diabetes show strong associations for its potential anticancer abilities. It is generally agreed upon that metformin acts mainly on the mitochondria, and we show evidence to support this through both cellular imaging and analysis of mitochondrial membrane lipids.

The major proposed targets of metformin are mitochondrial glycerol-3-phosphate dehydrogenase (mGPDH), complex 1, and AMP-activated protein kinase (AMPK). However, we show that these targets are highly dependent on cell type and nutrient availability, and downstream effects such as altered lipid metabolism may still be seen without significant alteration in the expression of these proteins.

Investigating the Mechanisms of Action of Metformin at Pharmacological Dose

by

Safiyyah Abdelhak Motaib

A Thesis Submitted to the Graduate Faculty of
North Carolina State University
in Partial Fulfillment of the
Requirements for the Degree of
Master of Science

Biochemistry

Under the Supervision of Dr. Xiaojing Liu

Raleigh, North Carolina

2021

APPROVED BY:

Dr. Xiaojing Liu

Dr. Robert Rose

Dr. Joseph Barycki

ACKNOWLEDGMENTS

I would like to thank my advisor, Dr. Xiaojing Liu, for the support, advice, and guidance she has provided throughout my time in her lab. I remember emailing her shortly after being accepted into the IBMP program regarding my interest in her lab, and from day one she was receptive and encouraging.

I also want to thank Dr. Robert Rose and Dr. Greg Buhrman for their immense moral support throughout my time as an IBMP student, and especially in the first year when everything was new and there were many uncertainties. I also want to thank them for putting the effort in starting this program, without which I probably would not have had the financial ability to obtain a degree in higher education.

Finally, I want to thank my lab members, neighboring lab members, and other peers for their support, company, and encouragement. I especially want to thank Dr. Likun Duan for his training and expertise, as well as Grace, Mareca, Emily, and Monica for just being there and friends and coworkers.

TABLE OF CONTENTS

LIST OF TABLES

LIST OF FIGURES

CHAPTER 1: INTRODUCTION

1.1. Why Metformin?

Metformin is a biguanide anti-diabetic pharmaceutical drug that has been successfully used for over thirty years. Despite its widespread use, metformin's primary mechanism of action is unclear. It is well established that metformin's anti-diabetic effects largely stem from its ability to inhibit hepatic glucose production, but the molecular pathways it takes to have these effects is controversial.[1,2,3,6,9] Much of this controversy comes from numerous *in vitro* analyses that use supra-pharmacological doses of metformin and are therefore observing exaggerated effects of metformin, which are not observed *in vivo* or at pharmacologically relevant doses *in vitro.*[1,2,9] The biguanide's ability to safely manage hyperglycemia is indisputable, but it has also been shown to have pleiotropic effects, including decreasing food intake and body weight, decreasing the risk of cardiovascular disease, altering lipid profile, modulating inflammatory markers, and possibly reducing cancer risk.[2, 3]

Metformin is a polar and hydrophilic compound, and therefore relies on organic cation membrane transporters (OCTs) to enter the cell.[8] It has been shown to be a weak inhibitor of the mitochondrial respiratory chain, which is more than likely a significant reason for the large variation in experimental results regarding metformin's molecular mechanisms. Unlike the similar but structurally variant biguanide phenformin, which is a strong inhibitor of the mitochondrial respiratory chain, metformin's molecular mechanisms seem to be more subtle and variable. Phenformin was also used as an anti-diabetic pharmaceutical but was taken off the market due to health concerns, mainly lactic acidosis, not seen with metformin treatment.[2,9]

Metformin's success as an anti-diabetic drug has made it an extremely commonly prescribed drug for hyperglycemia management. The sheer number of patients that have been taking the drug over the past few decades has resulted in the collection of a large amount of epidemiological data. Observational studies looking at patients who are prescribed metformin for diabetes showed that these patients had a lower incidence of cancer or were less likely to die from pre-existing cancer[3]. Metformin has also been shown to accumulate in tumors from ovarian cancer patients, where glucose concentrations can be as low as 1mM.[2] The combination of metformin and low glucose within tumors, may prevent the tumor cells from promoting an adaptive response to resist metformin induced stress. The key to understanding metformin's mechanisms of action may be in trying to understand this adaptive response.

1.2. Proposed mechanisms of action

How metformin is able to manage symptoms of hyperglycemia is still somewhat of a mystery. Although there is evidence suggesting metformin targets complex 1, mitochondrial glycerophosphate dehydrogenase (mGPDH), and AMPK, the evidence is conflicting.[1,2,3,5] The source of this disagreement largely stems from 1) the lack of convincing subcellular localization information and 2) the use of supra-pharmacological doses of metformin, where it inhibits complex 1 and mGPDH significantly. Attempts at quantifying metformin localization within different organelles have been made primarily using subcellular fractionation using gradient centrifugation techniques; however, small, water-soluble molecules such as metformin tend to diffuse out during cell handling especially with many washing and centrifugation steps.[21]

Furthermore, when pharmacologically relevant doses of metformin are used *in vivo*, differences in cell type and alteration of the cellular environment result in varying, and often conflicting experimental results.[2,4,5] In liver cells for example, evidence may suggest that metformin inhibits gluconeogenesis independent of complex 1, AMPK, acetyl-CoA carboxylase activity, or any significant increase in gluconeogenic enzyme expression. However, metformin did significantly alter glucose production from lactate and glycerol, indicating an increased cytosolic redox state as a result of metformin treatment. This, along with further protein analysis and knockout experiments indicated that metformin's main target in hepatic tissue *in vivo* is mGPDH.[1] Similarly, there is data to suggest that mGPDH is metformin's target in thyroid cancer both *in vitro* and *in vivo.* It was found that metformin downregulates mGPDH expression and inhibits oxidative phosphorylation. The same paper suggests a novel finding that mGPDH is an important regulator of thyroid cancer growth and metabolism and can be effectively targeted.[4]

However, in HEYA8 cells, ovarian cancer cell line, metformin did not seem to significantly alter mGPDH levels, but did target carbon metabolism nonetheless, and was shown to alter mitochondrial fuel usage and shift cellular redox and energy status. Metformin was also shown to limit the formation of TCA intermediates, cause NADH accumulation, and promote increased reactive oxygen species (ROS).[2,7] Furthermore, cells were able to be rescued from metformin induced death by supplementation with mitochondrial substrate or nutrients that produce downstream metabolites, indicating that under ideal environmental conditions, cells are able to adapt to metformin treatment. While metabolic changes are still seen under non-cancerous conditions, significant cell death is only observed in cancer cells or in cells exposed to limited metabolic substrate or nutrients.[2, 7, 8]

Although often difficult to detect, there is evidence that metformin alters NADH/NAD+ ratios within the cell. However, it is difficult to separate cytosolic redox status from mitochondrial redox status and therefore relative redox ratios are often inferred based on the ratios of NADH and NAD+ dependent reactions such as the malate aspartate shuttle and the ratios of 2-oxoglutarate and succinyl-CoA. In liver cells both *in vitro* and *in vivo*, metformin was shown to decrease glucose production only from substrates that rely on cytosolic NADH (lactate and glycerol) due to mGPDH inhibition.[1] This is, however, highly disputed due to claims that the malate-aspartate shuttle would be able to compensate for any effect on redox status due to mGPDH inhibition, therefore restoring cytosolic redox status. Enzymatic assays in pancreatic and liver cells failed to show direct inhibition of mGPDH. In fact, in their mGPDH knockout mice, NADH/NAD+ ratios were shown to be normal, therefore the idea that inhibition of mGPDH results in an altered cytosolic redox status may not be true.[9]

Metformin's relationship with AMPK is also highly disputed, with some research indicating AMPK activation after metformin treatment and others indicating otherwise. Once again, discrepancies in data are a result of varying concentrations of metformin treatment as well as differences in cell types.[2, 9] It was shown that metformin fails to improve symptoms of hyperglycemia in mice containing a knockout of the liver specific kinase LKB1, which catalyzes the phosphorylation of AMPK.[9, 10, 11] However, numerous other studies have failed to detect an increase in AMPK activation as a result of metformin treatment, and others have noted that metformin still presents hypoglycemic effects in AMPK and LKB1 knockout mice, therefore indicating that these effects are AMPK independent.[1, 5] Similarly, many cancers are unable to activate AMPK but are still susceptible to metformin's antiproliferative effects[11].

Complex 1 is also thought to be a major target of metformin, but once again there is conflicting evidence with some research indicating complex 1 inhibition due to metformin treatment and others failing to observe such effects. The apparent IC50 of isolated complex 1 was found to be between 19 and 79mM,[13] which is much higher than the concentration of metformin measured in plasma of both human and animal models, which is in the micromolar range. It is also unclear whether metformin accumulates within the mitochondria, or if its mechanism of action is indirect and does not necessarily require accumulation.[2] Metformin therefore is unlikely to directly inhibit complex 1 *in vivo,* rather it may target upstream signaling pathways, resulting in an amplified affect downstream.[13] However, despite metformin's ability to inhibit complex 1, it is unclear if this happens *in vivo*, and if it does, specific mechanisms may once again depend on cell type and nutrient availability.

The effects that metformin has on cellular lipid status have not been as thoroughly studied as metformin's ability to inhibit gluconeogenesis. Existing studies on lipid changes due to metformin treatment primarily focus on total triglyceride levels, which reflect metformin induced metabolic changes. However, there is not much data which looks at metformin induced alterations to mitochondrial membrane lipid profiles, especially through complex 1 inhibition. Considering that metformin is believed to act on the mitochondria, and mitochondrial membrane integrity and composition play an important role on mitochondrial function, evaluating these effects are important. Few attempts have been made to characterize metformin-induced lipid remodeling [22,23] such as membrane lipid alterations. Similar to controversy regarding protein targets of metformin and whether or not metformin's effects are AMPK dependent, questions regarding different doses of metformin and effects on lipid metabolism remain unanswered. Some studies find that metformin decreases fatty acid oxidation and leads to triglyceride accumulation [24] while other report increased rates of fatty oxidation.[25,26]

The one thing that is generally agreed up regarding metformin's mechanism of action is that the drug acts on the mitochondria.[4,8,9,10,13,] TCA intermediates and short chain acylcarnitines were the groups of compounds that were most often suppressed in tumors of metformin-treated patients[2]. It is well known that the TCA cycle provides substrate for numerous metabolic pathways and can serve as a major point of metabolic rewiring and regulation and is a central hub for both catabolic and anabolic pathways.[10] Therefore, in the presence of a metabolic inhibitor or as a result of limited nutrient availability, it is not surprising that TCA intermediates would be significantly altered. Metformin seems to cause a shift in lipid metabolism, and while some groups believe this results from AMPK activation, it is certainly possible that altered lipid metabolism due to metformin treatment is AMPK independent, and simply a result of metabolic rewiring through the TCA cycle.[2, 10]

Under conditions of limited glucose availability, cells (including tumor cells) tend to increase lipid catabolism in order to fuel the TCA cycle. However, increased fatty acid oxidation seems to make tumor cells more susceptible to metformin treatment, most likely due to the fact that lipid metabolism fuels the TCA cycle much slower than glucose metabolism[2]. Similarly, if AMPK is significantly activated due to metformin treatment, fatty acid oxidation increases due to downregulation of specific hepatic gene expression as well as a downregulation of acetyl-CoA carboxylase (ACC) activity.[10] Metformin could also alter lipid metabolism through complex 1 if inhibition indeed occurs. Rotenone, a well-known and strong inhibitor of complex 1, was shown to increase conversion of lipids to acetyl-CoA, therefore showing the potential for metformin to do the same.[14] Nonetheless, it is important to note that metformin, in theory, has the ability to alter lipid metabolism regardless of its effects on AMPK or complex 1 activity, simply as a result of inhibiting gluconeogenesis, but once again the mechanisms as to which metformin does so are unclear.

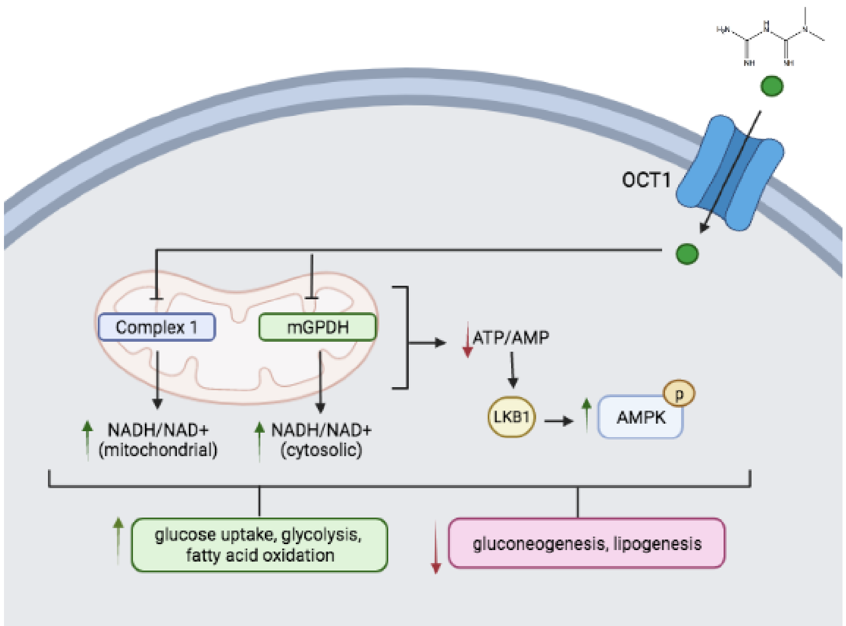

Figure 1.1. Simplified visualization of metformin's proposed mechanisms. Metformin enters the cell primarily via OCT1 and may inhibit complex 1 or mGPDH, resulting in altered redox status and potentially lowering cellular energy status, which can activate AMPK through LKB1 mediated phosphorylation. Metformin treatment may result in increased glucose uptake, glycolysis, and fatty acid oxidation and decreased gluconeogenesis and lipogenesis.

1.3. Evidence of metformin's anti-cancer effects

Despite the inability to pinpoint metformin's mechanisms of action in inhibiting gluconeogenesis, both epidemiological and experimental studies show convincing evidence that metformin has anti-cancer effects in addition to its well-known anti-diabetic properties. Various experiments seem to suggest that metformin can inhibit tumor proliferation under normal conditions and induce cell death under low glucose conditions.[2,8] The key to understanding how metformin works within the cell may be in elucidating why its effects vary under different environmental conditions and different cell types.

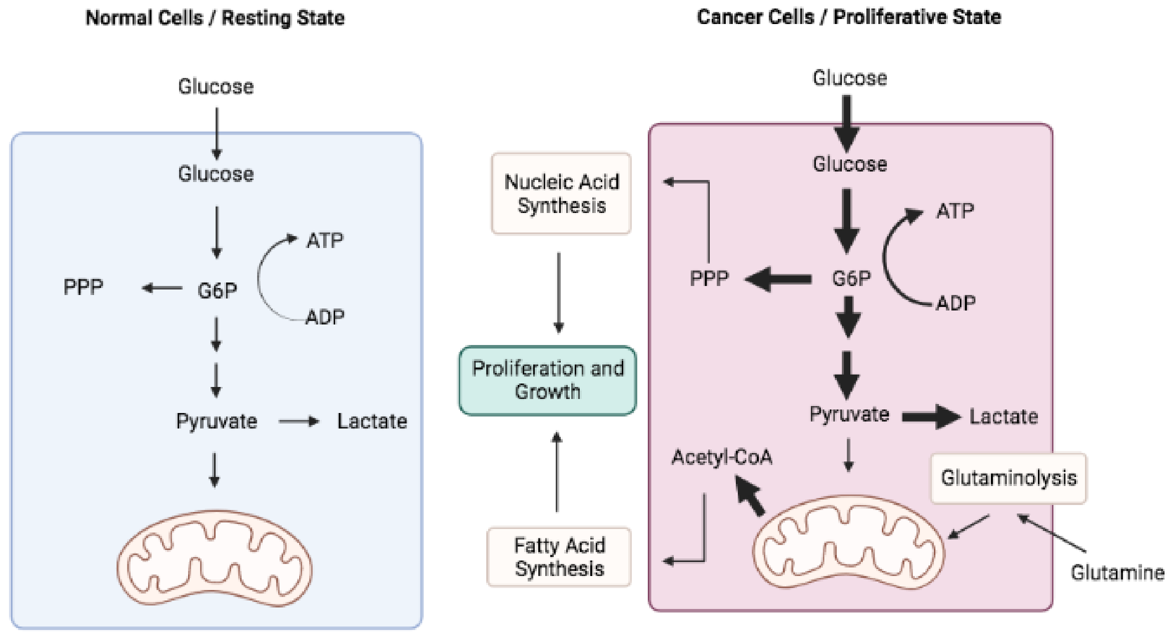

Figure 1.2. Differences in normal cell and cancer cell metabolism. In normal cells, glucose is metabolized to pyruvate and then completely oxidized to CO2 in the presence of oxygen. Only under limited oxygen does pyruvate get metabolized to lactate. However, cancer cells metabolize most of their lactate to pyruvate regardless of the presence of oxygen. The increased flux of glucose through glycolysis allows for the generation of excess intermediates such as glucose-6-phosphate (G6P), which is used to synthesize nucleic acids through the pentose phosphate pathway (PPP). Rather than glucose fueling the TCA cycle and Oxidative phosphorylation in the mitochondria, glutamate produced from glutaminolysis is used. In turn, citrate is used to produce acetyl-CoA, which is then used for fatty acid production and lipid synthesis. The increased synthesis of nucleic acids and lipids promote excess proliferation and cancer cell growth.[15,16]

Initial evidence of metformin's potential anti-cancer abilities came from epidemiological studies of diabetes patients treated with metformin, which showed an association between metformin treatment and a reduced risk of cancer.[16] One specific study found a strong association between metformin treatment and longer survival in patients chemotherapy with stage III-IV or recurrent endometrial cancer.[20] Further evidence of metformin's anti-cancer properties comes from numerous experimental studies *in vitro* and *in vivo*. Considering that metformin has been shown to target mitochondrial metabolism, it is important to consider the mitochondria's role in cancer progression and which pathways may be targeted for potential cancer therapy. Scientists studying cancer metabolism prior to the 1950s widely believed that mitochondria in tumor cells are damaged, resulting in high levels of DNA damaging ROS and forcing cancer cells to produce energy through oxidative glycolysis. However, as scientific methods advanced and further research was conducted, this notion was refuted. It was shown that cancer cell metabolism was similar to that seen in neoplastic cells, that mitochondrial activity is similar in both cancer and normal cells, and that fatty acids are still being oxidized via ß-oxidation pathways.[17,18] Similarly, metformin's potential to increase AMPK phosphorylation through LKB1 may be a promising pathway in which metformin inhibits cancer proliferations considering that LKB1 is a known tumor suppressor.[18,20]

Metformin's anti-cancer properties have been reported in thyroid cancer, gynecological cancers, and endometrial cancers. Numerous investigators have reported a dose-dependent inhibition of growth in endometrial cancer cell lines with metformin treatment.[2,20] Additionally, under limited glucose, metformin induces increased cell death of cancer cells but not of normal cells.[2,8,20]

1.4. Impact and research goals

The dispute over metformin's specific molecular mechanisms might largely be due to the drug's inherent mechanism of action, unlike the related phenformin, which has been shown to be toxic. This makes sense since strong inhibition of enzymes such as complex 1 or mGPDH, and strong activation of AMPK, would severely disrupt cellular homeostasis and would be unlikely to be the result of a drug deemed as safe, such as metformin. Additionally, despite our inability to pinpoint metformin's mechanism of action, the numerous epidemiological and experimental studies, both *in vitro* and *in vivo*, provide evidence that metformin has enormous potential as an anti-cancer agent. However, because different investigators report different targets of metformin, and cells from various tumor types seem to respond differently, making a specific claim as to what metformin can do.

In this study we investigate the molecular mechanisms of pharmacologically relevant doses of metformin in proliferating and non-proliferating cells. We will investigate the previously reported relationships between metformin, AMPK, mGPDH, and complex 1 through proteomic and metabolomic analyses. We also hope to use LCMS to determine the shift, if any, and mitochondrial lipid profiles due to mitochondrial adaptation to metformin treatment.

References

1. Madiraju, A. K.; Qiu, Y.; Perry, R. J.; Rahimi, Y.; Zhang, X.-M.; Zhang, D.; Camporez, J.-P. G.; Cline, G. W.; Butrico, G. M.; Kemp, B. E.; Casals, G.; Steinberg, G. R.; Vatner, D. F.; Petersen, K. F.; Shulman, G. I. Metformin Inhibits Gluconeogenesis via a Redox-Dependent Mechanism in Vivo. Nat Med 2018, 24 (9), 1384–1394. https://doi.org/10.1038/s41591-018-0125-4.

2. Liu, X.; Romero, I. L.; Litchfield, L. M.; Lengyel, E.; Locasale, J. W. Metformin Targets Central Carbon Metabolism and Reveals Mitochondrial Requirements in Human Cancers. Cell Metabolism 2016, 24 (5), 728–739. https://doi.org/10.1016/j.cmet.2016.09.005.

3. Pernicova, I.; Korbonits, M. Metformin—Mode of Action and Clinical Implications for Diabetes and Cancer. Nat Rev Endocrinol 2014, 10 (3), 143–156. https://doi.org/10.1038/nrendo.2013.256.

4. Thakur, S.; Daley, B.; Gaskins, K.; Vasko, V. V.; Boufraqech, M.; Patel, D.; Sourbier, C.; Reece, J.; Cheng, S.-Y.; Kebebew, E.; Agarwal, S.; Klubo-Gwiezdzinska, J. Metformin Targets Mitochondrial Glycerophosphate Dehydrogenase to Control Rate of Oxidative Phosphorylation and Growth of Thyroid Cancer In Vitro and In Vivo. Clin Cancer Res 2018, 24 (16), 4030–4043. https://doi.org/10.1158/1078-0432.CCR-17-3167.

5. Li, M.; Li, X.; Zhang, H.; Lu, Y. Molecular Mechanisms of Metformin for Diabetes and Cancer Treatment. Front. Physiol. 2018, 9, 1039. https://doi.org/10.3389/fphys.2018.01039.

6. Pecinová, A.; Brázdová, A.; Drahota, Z.; Houštěk, J.; Mráček, T. Mitochondrial Targets of Metformin—Are They Physiologically Relevant? BioFactors 2019, 45 (5), 703–711. https://doi.org/10.1002/biof.1548.

7. Rattan, R.; Graham, R. P.; Maguire, J. L.; Giri, S.; Shridhar, V. Metformin Suppresses Ovarian Cancer Growth and Metastasis with Enhancement of Cisplatin Cytotoxicity In Vivo. Neoplasia 2011, 13 (5), 483-IN28. https://doi.org/10.1593/neo.11148.

8. Wheaton, W. W.; Weinberg, S. E.; Hamanaka, R. B.; Soberanes, S.; Sullivan, L. B.; Anso, E.; Glasauer, A.; Dufour, E.; Mutlu, G. M.; Budigner, G. S.; Chandel, N. S. Metformin Inhibits Mitochondrial Complex I of Cancer Cells to Reduce Tumorigenesis. eLife 2014, 3, e02242. https://doi.org/10.7554/eLife.02242.

9. MacDonald, M. J.; Ansari, I. H.; Longacre, M. J.; Stoker, S. W. If Metformin Inhibited the Mitochondrial Glycerol Phosphate Dehydrogenase It Might Not Benefit Diabetes; preprint; Biochemistry, 2020.

10. Zhou, G.; Myers, R.; Li, Y.; Chen, Y.; Shen, X.; Fenyk-Melody, J.; Wu, M.; Ventre, J.; Doebber, T.; Fujii, N.; Musi, N.; Hirshman, M. F.; Goodyear, L. J.; Moller, D. E. Role of AMP-Activated Protein Kinase in Mechanism of Metformin Action. J. Clin. Invest. 2001, 108 (8), 1167–1174. https://doi.org/10.1172/JCI13505.

11. Febbraro, T.; Lengyel, E.; Romero, I. L. Old Drug, New Trick: Repurposing Metformin for Gynecologic Cancers? Gynecologic Oncology 2014, 135 (3), 614–621. https://doi.org/10.1016/j.ygyno.2014.10.011.

12. Storozhuk, Y.; Hopmans, S. N.; Sanli, T.; Barron, C.; Tsiani, E.; Cutz, J.-C.; Pond, G.; Wright, J.; Singh, G.; Tsakiridis, T. Metformin Inhibits Growth and Enhances Radiation Response of Non-Small Cell Lung Cancer (NSCLC) through ATM and AMPK. Br J Cancer 2013, 108 (10), 2021–2032. https://doi.org/10.1038/bjc.2013.187.

13. Fontaine, E. Metformin-Induced Mitochondrial Complex I Inhibition: Facts, Uncertainties, and Consequences. Front. Endocrinol. 2018, 9, 753. https://doi.org/10.3389/fendo.2018.00753.

14. Worth, A. J.; Basu, S. S.; Snyder, N. W.; Mesaros, C.; Blair, I. A. Inhibition of Neuronal Cell Mitochondrial Complex I with Rotenone Increases Lipid β-Oxidation, Supporting Acetyl-Coenzyme A Levels. Journal of Biological Chemistry 2014, 289 (39), 26895–26903. https://doi.org/10.1074/jbc.M114.591354.

15. Pavlova, N. N.; Thompson, C. B. The Emerging Hallmarks of Cancer Metabolism. Cell Metabolism 21.

16. Evans, J. M. M.; Donnelly, L. A.; Emslie-Smith, A. M.; Alessi, D. R.; Morris, A. D. Metformin and Reduced Risk of Cancer in Diabetic Patients. BMJ 2005, 330 (7503), 1304–1305. https://doi.org/10.1136/bmj.38415.708634.F7.

17. Zong, W.-X.; Rabinowitz, J. D.; White, E. Mitochondria and Cancer. Molecular Cell 2016, 61 (5), 667–676. https://doi.org/10.1016/j.molcel.2016.02.011.

18. Weinberg, S. E.; Chandel, N. S. Targeting Mitochondria Metabolism for Cancer Therapy. Nat Chem Biol 2015, 11 (1), 9–15. https://doi.org/10.1038/nchembio.1712.

19. Dowling, R. J. O.; Lam, S.; Bassi, C.; Mouaaz, S.; Aman, A.; Kiyota, T.; Al-awar, R.; Goodwin, P. J.; Stambolic, V. Metformin Pharmacokinetics in Mouse Tumors: Implications for Human Therapy. Cell Metabolism 2016, 23 (4), 567–568. https://doi.org/10.1016/j.cmet.2016.03.006.

20. Ezewuiro, O.; Grushko, T. A.; Kocherginsky, M.; Habis, M.; Hurteau, J. A.; Mills, K. A.; Hunn, J.; Olopade, O. I.; Fleming, G. F.; Romero, I. L. Association of Metformin Use with Outcomes in Advanced Endometrial Cancer Treated with Chemotherapy. PLoS ONE 2016, 11 (1), e0147145. https://doi.org/10.1371/journal.pone.0147145.

21. Arrivault, S.; Guenther, M.; Florian, A.; Encke, B.; Feil, R.; Vosloh, D.; Lunn, J. E.; Sulpice, R.; Fernie, A. R.; Stitt, M.; Schulze, W. X. Dissecting the Subcellular Compartmentation of Proteins and Metabolites in Arabidopsis Leaves Using Non-Aqueous Fractionation. Molecular & Cellular Proteomics 2014, 13 (9), 2246–2259. https://doi.org/10.1074/mcp.M114.038190.

22. Miklankova D, Markova I, Huttl M, Zapletalova I, Poruba M and Malinska H. Metformin Affects Cardiac Arachidonic Acid Metabolism and Cardiac Lipid Metabolite Storage in a Prediabetic Rat Model. Int J Mol Sci. 2021;22.PMC8305829

23. Kim W, Deik A, Gonzalez C, Gonzalez ME, Fu F, Ferrari M, Churchhouse CL, Florez JC, Jacobs SBR, Clish CB and Rhee EP. Polyunsaturated Fatty Acid Desaturation Is a Mechanism for Glycolytic NAD(+) Recycling. Cell Metab. 2019;29:856-870 e7.PMC6447447

24. Corsini GU, Sirigu F, Tagliamonte P and Muntoni S. Effects of biguanides on fatty acid and glucose oxidation in muscle. Pharmacol Res Commun. 1974;6:253-61

25. Collier CA, Bruce CR, Smith AC, Lopaschuk G and Dyck DJ. Metformin counters the insulin-induced suppression of fatty acid oxidation and stimulation of triacylglycerol storage in rodent skeletal muscle. Am J Physiol Endocrinol Metab. 2006;291:E182-9

26. Gonzalez-Barroso MM, Anedda A, Gallardo-Vara E, Redondo-Horcajo M, Rodriguez-Sanchez L and Rial E. Fatty acids revert the inhibition of respiration caused by the antidiabetic drug metformin to facilitate their mitochondrial beta-oxidation. Biochim Biophys Acta. 2012;1817:1768-75

CHAPTER 2: METFORMIN INDUCED CELL DEATH AND METFORMIN CELLULAR LOCALIZATION

2.1. Abstract

Metformin has been used to treat hyperglycemia for decades; but recent epidemiological studies have seen associations that suggest metformin has anti-cancer properties as well. Despite years of use and hundreds of scientific journal articles written, metformin's mechanisms of action are yet to be elucidated. A major flaw in many of the past experimental analyses have been that claims were made using supra-pharmacological doses of metformin which is not representative of *in vivo* plasma concentrations.[1,2,3] We conducted immunofluorescence analysis using a click chemistry compatible metformin analogue, which allowed us to visualize the localization of metformin within the cell under various, pharmacologically relevant doses and in cancerous HEYA8 cells, proliferating C2C12 cells and non-proliferative C2C12 myotubes.

2.2. Introduction

Metformin is a very popular pharmaceutical biguanide that has been effectively used to treat hyperglycemia for decades. Yet its molecular mechanisms are poorly understood despite over 17,000 articles regarding metformin on PubMed. Among numerous laboratories investigating metformin, the vast majority seem to agree that metformin acts on the mitochondria or at the very least mitochondrial enzymes; but whether or not this effect requires accumulation within the mitochondria or not, has not been agreed upon.[1,2,3] Although some investigators report that metformin does not inhibit complex one, others show that low doses (in the micromolar range) can result in significant complex 1 inhibition. However, it takes supra-pharmacological doses (in the millimolar range) to inhibit complex 1 in isolated mitochondria.[2,3] To explain this, many hypothesize that metformin does indeed have a direct effect on the mitochondria, possibly even accumulating, while others report that metformin may induce a cell signaling pathway that is lost when mitochondria are isolated.[2]

It has also been shown that metformin inhibits growth in cancer cells under low glucose conditions, indicating that the drug forces these cells to rely on glycolysis rather than oxidative phosphorylation, which occurs within the mitochondria. Metformin may, either directly or indirectly, be disrupting the energy supply produced by mitochondria within cancer cells by targeting mitochondrial metabolism.[4] The combination of metformin induced mitochondrial stress and limited substrate availability, may prevent cancer cells from triggering an adaptive response that allows for metabolic adaptation to metformin induced stress. In order to attempt to understand metformin's mechanisms of actions, we first looked at whether or not metformin colocalizes with the mitochondria. To do this we collaborated Dr. Wei-chen Chang's lab at North Carolina State University to develop a drug surrogate to metformin, which is phenotypically identical and can be labeled in situ using click chemistry protocols.[5]

Click chemistry is a simple and powerful tool that allows for the visualization of small molecules within biological samples [6,8]. While it isn't without limitations, click chemistry can be used for a variety of different biochemical applications including high-throughput screening, fragment based drug discovery, enzyme inhibitor development, receptor-ligand binding studies, and in situ chemistry. It has also been shown that click chemistry produces stable products without any byproducts, and are highly tolerant under physiological conditions such as high presence of oxygen and water. [6,7,8] The chemical reaction itself involves the chemical reaction starting with a terminal acetylene and ending with the formation of a 1,2,3-triazole catalyzed by copper(I) **(figure 2.2A)**.

This protocol allows us to visualize metformin localization within the cell with as little disruption as possible. Considering metformin's solubility and our hypothesis that metformin, under pharmacologically relevant doses, makes weak interactions within the cell, this method seemed most appropriate. Subcellular fractionation poses the risk of small molecule leakage during the many, high speed, centrifugation steps, which will likely alter metformin levels detected as well as potential cross-contamination of organelles and improper separation.[9,10, 11, 13]

2.3. Results

Metforminyn, which we will refer to as metformin's clickable analogue, was synthesized by Dr. Wei-chen Chang's lab at North Carolina State University to develop a drug surrogate to metformin **(figure 2.1A)** and checked for purity by H NMR **(figure2.1B)** and ^{13}C NMR **(figure2.1C)**.

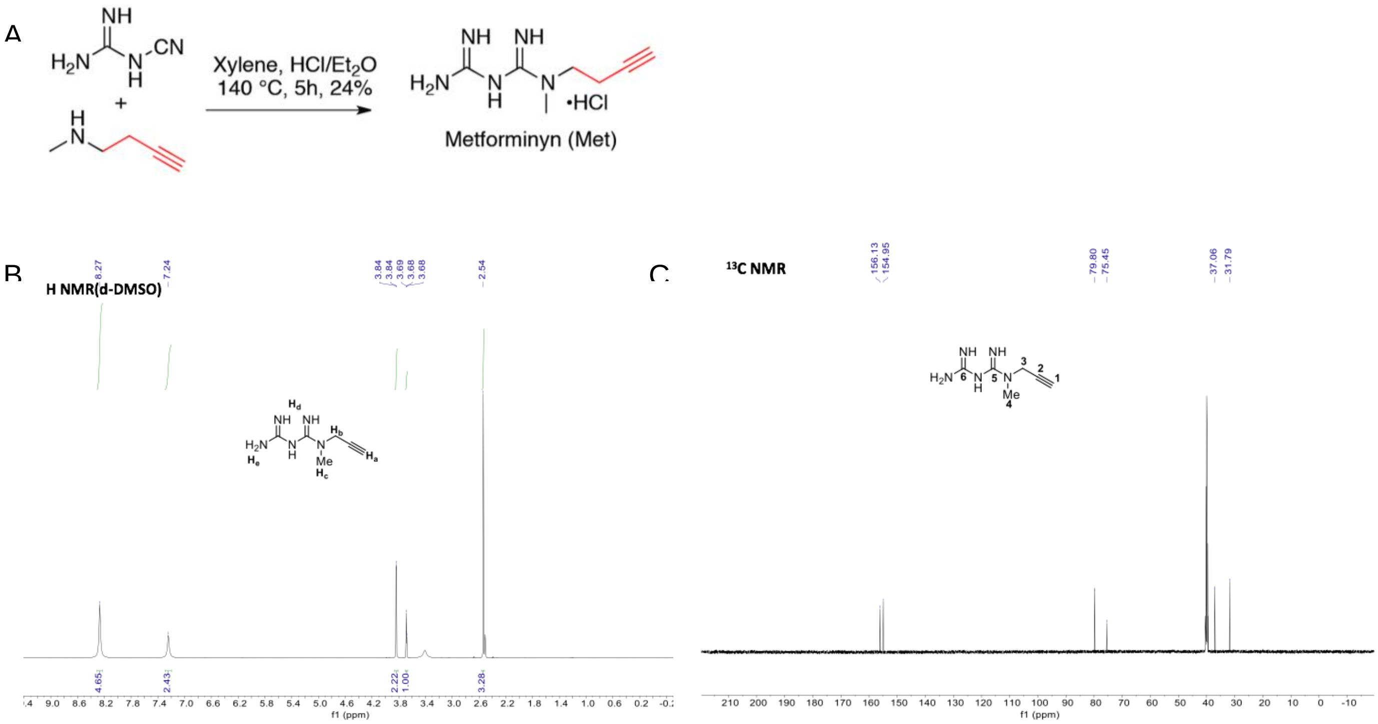

Figure 2.1. Clickable metformin analogue synthesis. Clickable metformin (metforminyn) formation reaction (A), H NMR (B) and 12C NMR (C) analysis of final product. Synthesis and NMR analysis conducted by Dr. Wei-Chen Chang's lab at North Carolina State University.

We first conducted an MTT assay to ensure that the clickable metformin analogue has similar effects on cells and does not significantly alter cell death. Our findings were that the analogue did not affect cell death under normal glucose conditions and decreased cell viability under low glucose conditions, which is characteristic of metformin **(figure 2.2)**. We therefore proceeded with click chemistry analysis with confidence that the analogue accurately represents metformin's physical location when imaged.

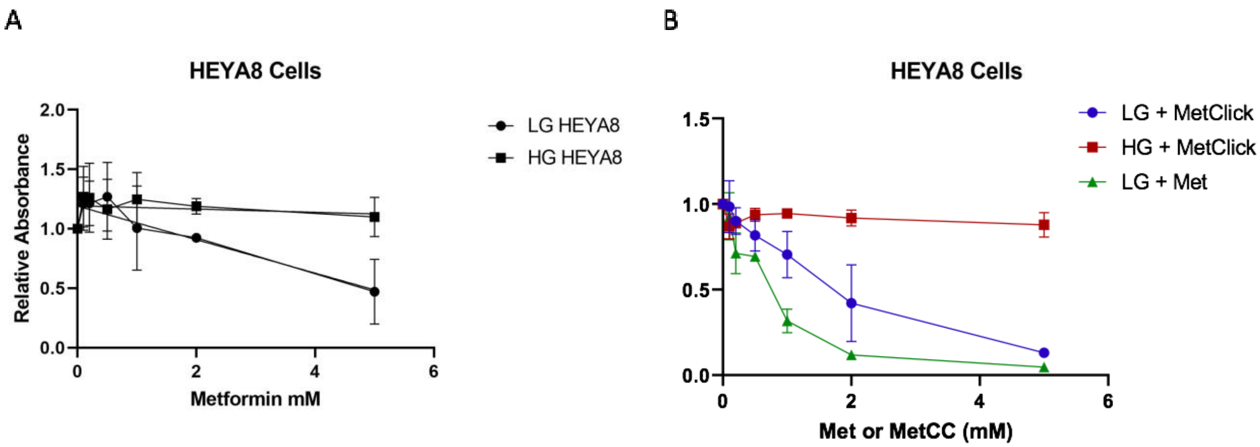

Figure 2.2. MTT Cell Viability Assay. Analysis of cell viability with increasing doses of metformin under high and low glucose conditions (A) and of clickable metformin analogue under high and low glucose conditions and metformin under low glucose conditions (B).

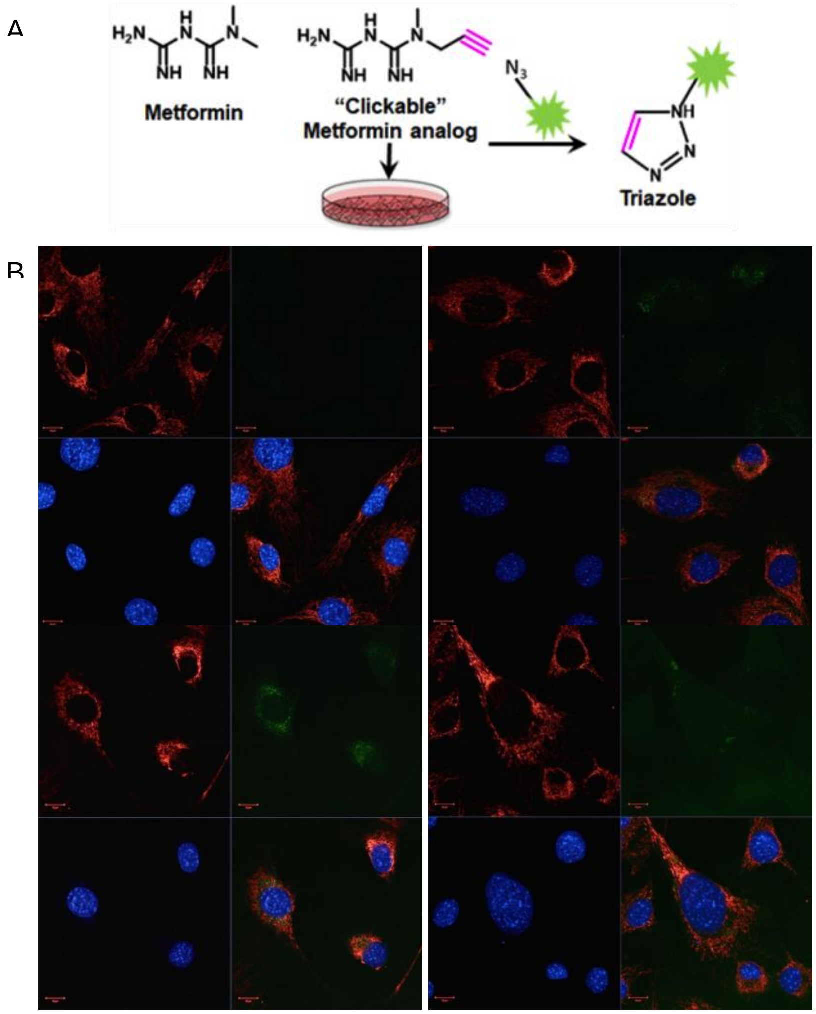

Figure 2.3. C2C12 metformin cellular localization analysis. Schematic of click chemistry triazole formation using synthesized clickable metformin analogue (A). Nucleus (DAPI blue), clickable metformin analogue (green), metformin (red), and an overlay of cells treated with 0 uM (top left), 40uM (top right), 120 uM (bottom left) and 200uM (bottom right). Images taken under a confocal microscope by NCSU Microscopy (B).

Immunofluorescence images of C2C12 undifferentiated myocytes show a strong signal for metformin at 120 uM and 200 uM metformin, and the drug's colocalization with the mitochondria is especially evident at 120 uM **(figure 2.3)**. It may be beneficial to conduct quantitative analyses in order to say for certain whether or not metformin accumulates within the mitochondria in these cells. This would simply require setting up the experiment so that one slide contains only one fluorophore, to ensure no contamination of fluorescent signal under the microscope.

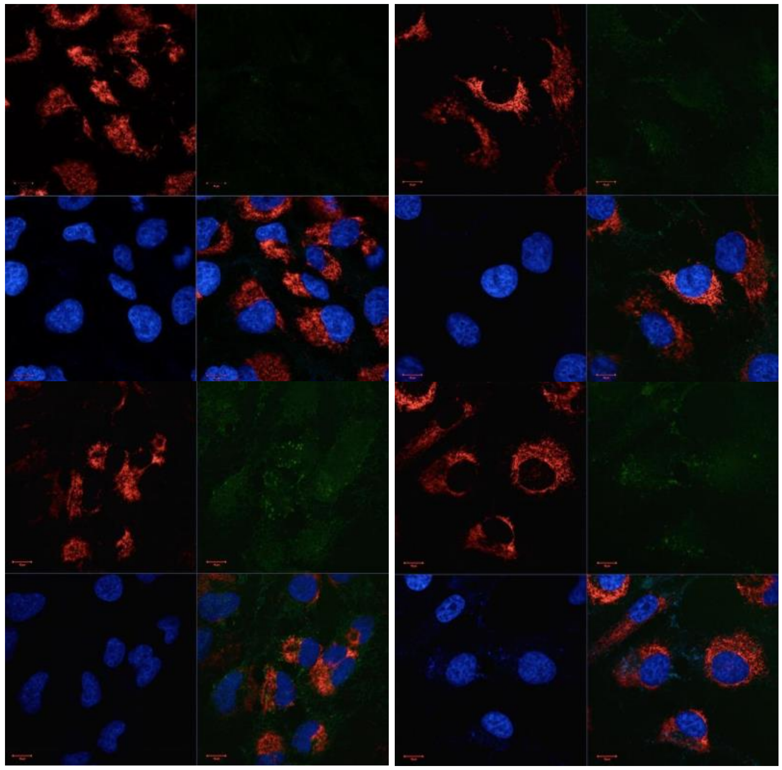

Figure 2.4. HEYA8 metformin cellular localization analysis. Nucleus (DAPI blue), clickable metformin analogue (green), metformin (red), and an overlay of cells treated with 0 uM (top left), 40uM (top right), 120 uM (bottom left) and 200uM (bottom right). Images taken under a confocal microscope by NCSU Microscopy.

The images of HEYA8 cells provided less convincing evidence of metformin accumulation within the mitochondria, but there does seem to be some colocalization **(figure 2.4)**. Once again, quantitative analyses may be of benefit to accurately determine the extent of which metformin does or doesn't accumulate within the mitochondria. However, in C2C12 differentiated myotubes, we see no evidence of any accumulation or colocalization **(figure 2.5)**.

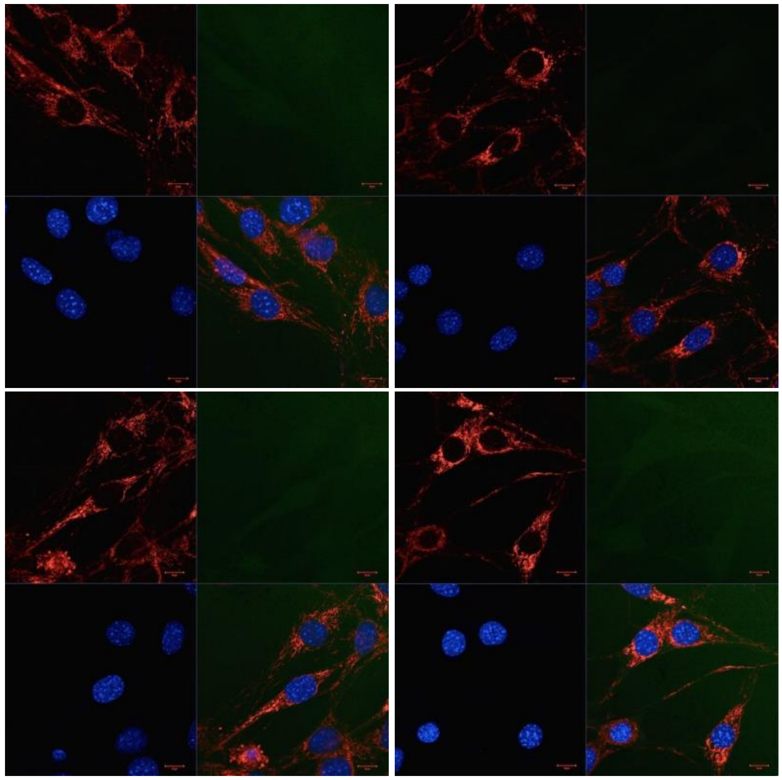

Figure 2.5. C2C12 differentiated myotube metformin cellular localization analysis. Nucleus (DAPI blue), clickable metformin analogue (green), metformin (red), and an overlay of cells treated with 0 uM (top left), 40uM (top right), 120 uM (bottom left) and 200uM (bottom right). Images taken under a confocal microscope by NCSU Microscopy.

2.4. Discussion

These results also show the importance of evaluating various cell types and give insight into why different research groups have such varying conclusions regarding metformin and its molecular mechanisms. A lack of visible metformin accumulation or localization in the C2C12 myotubes may be due to multiple factors including but not limited to these cells' tendency to have a much higher metabolic rate and to have significantly increased mitochondrial numbers. This may allow them to quickly metabolize metformin, making it difficult to visualize metformin.

Future studies should be conducted to attempt to quantify any spatial associations between metformin and the mitochondria. We attempted to do so but did not have the time to set up the proper controls to ensure proper quantification through the software. We also attempted to capture metformin induced morphological changes to the mitochondria but were unable to get images with reasonable resolution. This may be due to our choice to label cytochrome C as a mitochondrial marker, which seems to be a better choice for identifying mitochondrial tubules, junctions and endpoints, especially with a confocal microscope.

However, it is important to keep in mind that mitochondrial size and shape are highly variable even within the same cell let alone among neighboring cells in the same treatment group and cells from different treatment groups. [9] Considering that we find metformin to be a weak complex 1 inhibitor, any mitochondrial stress that does occur may not be drastic enough to provide reliable morphology data. Although our results don't tell us anything about whether metformin specifically targets mitochondrial enzymes, it helps to reassure that metformin can accumulate within the cell, and even enter the mitochondria.

2.5. Materials and Methods

Table 1. Chapter 2 materials list. List of materials used to conduct experiments for Chapter 2

Antibodies	Product	Source	Identifier
	Anti-rabbit IgG Alexa Fluor 594 Conjugate	Cell Signaling	8889S
	Cytochrome c (6H2.B4) Mouse mAb	Cell Signaling	12963S

Commercial Assays	Product	Source	Identifier
	Click-iT™ EdU Alexa Fluor™ 488 Imaging Kit	Invitrogen	REF C10337

Instruments and Software	Product	Source	Identifier
	Zeiss LSM 880	NC state microscopy	NA
	Zeiss Zen Lite Software	Zeiss	NA
	Cytation 5 Imaging Reader	BioTek	NA

Reagents and Resources	Product	Source	Identifier
	Cellview glass bottom cell culture dish	greiner bio one	627870
	Dulbecco's Modified Eagle Medium (DMEM)	Corning	10-017-CV
	Horse serum	Corning	35-030-cv
	MTT	Invitrogen	M6494
	Phenol Red Free RPMI-1649 Cell Medium	Sigma Aldrich	R7509
	ProLong ™ Gold Antifade Reagent with DAPI	Invitrogen	REF P36935

Table 1 (continued)			
	Triton ™ X-100	VWR	0694-1L
	clickable metformin		NA
	10X Dulbecco's PBS	MP Bio	1960454
	100 X 15mm Petri Dish	VWR	25384-302
	15 mL Centrifuge Tubes	VWR	Cat. No. 525-0401
	1mL disposable syringes luer tip	Air-Tite	MS1
	250 mL 0.22um Filter	Corning	431096
	50 mL Conical 0.22um Filter	VWR	89220-17
	6 well plates	TrueLine	TR5000
	Dialyzed FBS	gibco	26400-044
	FBS (Fetal Bovine Serum)	gibco	16000-044
	Glucose (C6H12O6)	Alfa Aesar	A16828
	Metformin Hydrochloride	TCI Chemicals	TCI-M2009 CAS 115-70-4
	N-Acetyl-L-Cysteine	MP Bio	1009005-200MG
	Non-Fat Dry Milk	Labscientific	Cat# M0841
	Pen Strep	ThermoFIsher Scientific	15070063
	RPMI 1640 Growth Medium	MP Bio	CAT NO. 1060126
	RPMI 1640 Growth Medium without glucose	Sigma Aldrich	R1383-10X1L
	Serum-Free Cell Freezing Medium	GC LTEC	Cat.No. 302-14681 (CS-02-001)

Table 1 (continued)			
	Sodium Hydrogen Carbonate (NaHCO3)	Alfa Aesar	A17005
	Sterile Syringe 0.2um Filter	VWR	28145-501
	trypsin	Corning	25-051-CI
	Cryo-Vials	Corning	430659

Cell Culture

All cells were cultured in 10 cm dishes with full growth medium containing RPMI 1640, 10% FBS, and 1% penicillin-streptomycin. All cells were incubated at 37ºC and 5% CO_2. Cells were split at 75% - 85% confluence at a 1:20 ratio and were discarded past the recommended number of passages. C2C12 cells were provided by the Tissue Culture Facility (TCF) at UNC Lineberger. HEYA8 OvCa cells were donated by Dr. Ernst Lengyel's lab at the University of Chicago. C2C12 myotubes were differentiated from C2C12 cells by incubation with DMEM and 2% horse serum for four days.

Cell Storage

Cells stored for later use were frozen at a concentration of 5 x 10^6 cells / mL in CELLBANKER® cryopreservation medium and frozen at -80 ºC until thawed for use.

Cell Viability Assay

Cell viability was assessed using a tetrazolium-based MTT assay. Cells were seeded in a 96 well plate at a concentration of 3000 cells per well and left overnight to adhere. Cells were then incubated with different concentrations of metformin for 48 hours at 37ºC and 5% CO_2. After treatment, the media was removed and replaced with 100uL of phenol red free RPMI and left to incubate for 1 hour before beginning the MTT assay. A 12mM MTT stock solution was prepared and 10uL of the solution was added into each well and cells were left to incubate for four hours. An SDS-HCl solution was made by adding 1g of SDS to 10mL of 0.01M HCl. After the initial incubation, 100uL of the SDS-HCl solution was added and left to incubate at 37º in a humidified incubator for two hours. Absorbance was read at 570 nm using BioTek's Cytation 5 Imaging Reader.

Clickable Metformin Synthesis

In a sealed tube, commercially available dicyandiamide (169 mg, 2.0 mmol) and N-methylbut-3-yn-1-amine (200 mg, 2.4 mmol) were suspended in 20 mL of xylene, then 2.5 mL of a 1 M aq. HCl solution were added. The tube was closed and heated at 140°C for 5 h. After this time, the reaction was cooled to RT and MeOH was added, then the solvent was removed under vacuum. The crude residue was purified by chromatography using a combiflash apparatus (DCM/MeOH, 10 to 20%) to produce Met as a white solid (97 mg, 24%). Synthesized by Dr. Wei-chen Chang's lab at North Carolina State University.

Immunofluorescence

On day 0, HEYA8 cells were seeded at 15,000 cells per well and incubated on a Cellview glass bottom cell culture dish. On day 1, cells were treated and left to incubate for 24 hours. On day 2, cells were incubated with clickable Metformin for 3 hours, and were then fixed with 2% formaldehyde in PBS for 12 minutes. After fixing, cells were permeabilized with 0.1% Triton X-100 in PCS for 10 minutes and then washed three times with 1% BSA in PBS. After washing, the cells were incubated in a 2% BSA, 0.2% tween blocking solution in PBS for 20 minutes at room temperature. Clickable metformin was synthesized by Dr. Wei-chen Chang's lab at North Carolina State University. Next, we used the Click-iT Edu imaging kit and followed the manufacturer's instructions in order to visualize metformin cellular localization. Cells were then incubated in the blocking buffer and incubated with 250uL of GPD2 anti-rabbit primary antibody diluted in the blocking buffer at a 1:300 ratio for 1 hour at room temperature. Cells were then washed three times in the blocking buffer and incubated with ALexa Fluor 594 conjugate for 1 hour at room temperature. Cells were washed three times with PBS and mounted using ProLong™ Gold Antifade Reagent with DAPI.

Confocal Microscopy

Images were acquired through NC State's Cellular and Molecular Imaging Facility who provided the training and instrumentation. The specific instrument used to obtain our images was the Zeiss LSM 880 Confocal System, and our lab was trained by Dr. Mariusz Zareba. Images were acquired with a 40x water immersion objective with a working distance of 600um. Acquisition wavelengths were set at 405nm, 488nm, and 561nm, and images were analyzed using Zen Lite 2012 Blue Edition. Images were taken under the following parameters: Scaling X: 0.090 um, scaling Y: 0.090 um. Dimensions x: 1180 y: 1180. Image size x: 106.27 um, 7: 106.27 um. Scan mode: plane. Objectives: LD C-Apochromat 40x/1.1 W Korr M27. Pixel dwell: 3.56 us. Master gain: 561 Ch52: 800, 488 Ch51: 800, 405 Ch1: 700. Digital gain: 561 Ch52: 1.00, 488 Ch51: 1.00, 405 Ch1: 1.00. Digital offset: 561 Ch52: 0.00, 488 Ch51: 0.00, 405 Ch1: 0.00. Pinhole: 561 Ch52: 40 um, 488 Ch51: 40 um, 405 Ch1: 40 um. Filters: 561 Ch52: 570-677, 488 Ch51: 508-561, 405 Ch1: 416-472. Beam splitters: MBS: MBS 488/561, MBS_InVis: MBS -405, DBS1: Mirror. Lasers: 561 561nm: 0.6000 %, 488 488 nm: 10.0 % , 405 405nm: 1.5 %

References

1. Fontaine, E. Metformin-Induced Mitochondrial Complex I Inhibition: Facts, Uncertainties, and Consequences. Front. Endocrinol. 2018, 9, 753. https://doi.org/10.3389/fendo.2018.00753.

2. Liu, X.; Romero, I. L.; Litchfield, L. M.; Lengyel, E.; Locasale, J. W. Metformin Targets Central Carbon Metabolism and Reveals Mitochondrial Requirements in Human Cancers. Cell Metabolism 2016, 24 (5), 728–739. https://doi.org/10.1016/j.cmet.2016.09.005.

3. Owen, M. R.; Doran, E.; Halestrap, A. P. Evidence That Metformin Exerts Its Anti-Diabetic Effects through Inhibition of Complex 1 of the Mitochondrial Respiratory Chain. 2000, 8.

4. Wheaton, W. W.; Weinberg, S. E.; Hamanaka, R. B.; Soberanes, S.; Sullivan, L. B.; Anso, E.; Glasauer, A.; Dufour, E.; Mutlu, G. M.; Budigner, G. S.; Chandel, N. S. Metformin Inhibits Mitochondrial Complex I of Cancer Cells to Reduce Tumorigenesis. eLife 2014, 3, e02242. https://doi.org/10.7554/eLife.02242.

5. Müller, S.; Versini, A.; Sindikubwabo, F.; Belthier, G.; Niyomchon, S.; Pannequin, J.; Grimaud, L.; Cañeque, T.; Rodriguez, R. Metformin Reveals a Mitochondrial Copper Addiction of Mesenchymal Cancer Cells. PLoS ONE 2018, 13 (11), e0206764. https://doi.org/10.1371/journal.pone.0206764.

6. Thirumurugan, P.; Matosiuk, D.; Jozwiak, K. Click Chemistry for Drug Development and Diverse Chemical− Biology Applications. Chem. Rev. 2013, 75.

7. Hein, C. D.; Liu, X.-M.; Wang, D. Click Chemistry, A Powerful Tool for Pharmaceutical Sciences. Pharm Res 2008, 25 (10), 2216–2230. https://doi.org/10.1007/s11095-008-9616-1.

8. Devaraj, N. K.; Finn, M. G. Introduction: Click Chemistry. Chem. Rev. 2021, 121 (12), 6697–6698. https://doi.org/10.1021/acs.chemrev.1c00469.

9. Harwig, M. C., Viana, M. P., Egner, J. M., Harwig, J. J., Widlansky, M. E., Rafelski, S. M., & Hill, R. B. (2018). Methods for imaging mammalian mitochondrial morphology: A prospective on mitograph. Analytical Biochemistry, 552, 81–99. https://doi.org/10.1016/j.ab.2018.02.022

10. Wang, Y.; An, H.; Liu, T.; Qin, C.; Sesaki, H.; Guo, S.; Radovick, S.; Hussain, M.; Maheshwari, A.; Wondisford, F. E.; O'Rourke, B.; He, L. Metformin Improves Mitochondrial Respiratory Activity through Activation of AMPK. Cell Reports 2019, 29 (6), 1511-1523.e5. https://doi.org/10.1016/j.celrep.2019.09.070.

11. Garbis, S.; Lubec, G.; Fountoulakis, M. Limitations of Current Proteomics Technologies. Journal of Chromatography A 2005, 1077 (1), 1–18. https://doi.org/10.1016/j.chroma.2005.04.059.

12. Rattan, R.; Graham, R. P.; Maguire, J. L.; Giri, S.; Shridhar, V. Metformin Suppresses Ovarian Cancer Growth and Metastasis with Enhancement of Cisplatin Cytotoxicity In Vivo. Neoplasia 2011, 13 (5), 483-IN28. https://doi.org/10.1593/neo.11148.

13. Arrivault, S.; Guenther, M.; Florian, A.; Encke, B.; Feil, R.; Vosloh, D.; Lunn, J. E.; Sulpice, R.; Fernie, A. R.; Stitt, M.; Schulze, W. X. Dissecting the Subcellular Compartmentation of Proteins and Metabolites in Arabidopsis Leaves Using Non-Aqueous Fractionation. *Molecular & Cellular Proteomics* **2014**, *13* (9), 2246–2259. https://doi.org/10.1074/mcp.M114.038190.

CHAPTER 3: ELUCIDATING METFORMIN'S MOLECULAR MECHANISMS UNDER PHARMACOLOGICALLY RELEVANT DOSES

3.1. Abstract

Metformin's popularity as an anti-diabetes therapeutic is well merited but the drug's molecular mechanisms are yet to be properly elucidated. It is generally agreed that metformin targets the mitochondria, and our previous imaging studies seem to suggest that this is true. Most research conducted on metformin's ability to systematically affect glucose metabolism points towards three main protein targets: mitochondrial glycerol 3-phosphate dehydrogenase (mGPDH), complex 1, and AMP-activated protein kinase (AMPK). We conduct immunoblotting after treating HEYA8 ovarian cancer cells, C2C12 myocytes, and C2C12 myotubes to determine whether or not these proteins are altered by metformin treatment and find that changes in mGPDH and complex 1 levels are cell type dependent, while none of these cells showed evidence of metformin induced AMPK activation. We further conduct liquid chromatography-mass spectroscopy (LCMS) to determine alterations in redox state and find that mitochondrial redox reactions showed evidence of increased production of reduced metabolites.

We also find that despite whether or not complex 1 expression is altered, fatty acid metabolism and overall lipid profiles are altered post metformin treatment.

3.2. Introduction

Despite metformin's widespread use as a first line treatment for hyperglycemia, the drug's mechanisms of action are unclear. Investigators seem to agree that metformin acts on the mitochondria to inhibit gluconeogenesis. However, this is the extent to which the scientific community has been able to elucidate metformin's molecular mechanisms. Among the major issues with previous research conducted on metformin is that experiments are conducted using supra pharmacological doses, which do not reflect plasma concentrations *in vivo*.[1,2,3] *In vitro* studies using isolated mitochondria require supra pharmacological doses of metformin (in the millimolar range) to see altered protein expression. However, plasma levels *in vivo* are in the micromolar range and in order to reliably determine metformin's molecular mechanisms, pharmacologically relevant doses must be used.[1,4,5,6]

In addition to metformin's indisputable ability to treat symptoms of hyperglycemia, investigators have begun to notice metformin's anticancer and anti-proliferative properties in certain cell types[1,3,7,12] Interestingly, metformin seems to affect cancerous, proliferative, and non-proliferative cells differently. While not much data exists examining metformin's effects on non-proliferative cells, many investigators report anti-proliferative effects in cancerous cells and even increased cell death under low glucose conditions.[1] It is well known that cancers have altered metabolism, a hallmark of which includes aerobic glycolysis also known as the Warburg effect, as well as limited vascular structure within tumors *in vivo* and therefore a limited supply of nutrients including glucose. Metformin's capacity for altering glucose metabolism likely contributes to its reduction of cell proliferation of cancerous cells, which are amplified under low glucose conditions. [1,12]

The drug's antiproliferative effects are thought to mainly be a result of inhibition of mGPDH, inhibition of Complex 1, and AMPK activation.[1] Some labs claim that metformin significantly inhibits mGPDH, which then increases NADH/NAD+ ratios and alters cellular redox state, eventually leading to limited energy production.[1,4,9] However, other labs contest this mechanisms due to the presence of the more abundant aspartate-malate shuttles which can easily compensate for increased NADH/NAD+ levels caused by mGPDH inhibition. Therefore, even if metformin does inhibit mGPDH, it may not be the main mechanism of action responsible for the drug's therapeutic effects.[1,8]

Similarly, the theory that metformin acts on complex 1 to increase NADH/NAD+ ratios and pAMPK/AMPK ratios is also disputed. The main issue with much of the data suggesting that complex 1 is significantly downregulated is the result of treating cells with supra pharmacological doses. [1,6] There is conflicting evidence as to whether AMPK activation is indeed increased after metformin inhibition.[1,10, 11] AMPK is a major regulator of both glucose and lipid metabolism, and while studies report increased AMPK activation in hepatic tissue, antiproliferative effects in other cell types are still seen without AMPK activation. In fact, the effects that metformin has on lipid metabolism may provide further clues as to what the drug is doing within the cell, and more specifically how mitochondrial function is altered.[1,10]

Mitochondrial function is heavily dependent on the integrity and composition of the mitochondrial membrane.[19] Proper biogenesis of the mitochondrial membrane requires a variety of complex protein and lipid complexes. While the different types of protein complexes are well studied and generally understood, the assembly of lipids and the way they interact with membrane proteins are not clear. Nevertheless, cardiolipins are known to be of extreme importance because of its ability to tightly bind to proteins, which allows the formation of superclusters.[13] Considering that complex 1 is the largest enzyme complex of the mitochondrial respiratory chain,[20] we hypothesize that cardiolipins play an important role in modulating complex 1 activity. Similarly, alterations in complex 1 which lead to the enzyme's overexpression may lead to protein crowding within the mitochondrial inner membrane. However, it is possible that a subsequent overproduction of cardiolipins can mediate negative effects of complex 1 overexpression by allowing the inner membrane to compensate for overcrowding of proteins. This would explain the mitochondria's ability to adjust to metabolic stress, and even change shape to accommodate high levels of stress.

Alteration in complex 1 activity has also been shown to be an important modulator of beta-oxidation and fatty acid metabolism. However, the exact relationship between complex 1 and lipid metabolism is disputed. For example, patients with complex 1 deficiency have been shown to have an accumulation of lipids due to impaired mitochondrial fatty acid oxidation,[21] while complex 1 inhibitors have been shown to increase fatty acid oxidation and decrease lipid stores.[22, 23]

Despite countless studies, there has yet to be a consensus amongst the scientific community regarding which, if any of these are metformin's main targets. It may also be that metformin acts on different enzymes under different cellular conditions and in different cell types. This would explain why investigators are unable to agree on what metformin's actions are *in vivo.* Understanding how metformin's effects seem to be amplified under low glucose conditions and noting phenotypic differences in non-proliferative cells after treatment may be the key to finally elucidating the drug's molecular mechanisms.

3.3. Results

We evaluated mGPDH and Complex 1 levels in HEYA8 ovarian cancer cells and found that mGPDH levels were decreased under low glucose conditions but not due to metformin treatment **(figure 3.1A).** However, complex 1 expression was significantly increased only under low glucose conditions, indicating that these cancerous cells are not able to compensate and recover from metformin induced stress when glucose is limited **(figure 3.1B).** It is likely that in these cells, metformin targets the mitochondria, where both glucose metabolism and oxidative phosphorylation occur. We then went on to evaluate whether this compensation by complex 1 overexpression can be mediated by restoration of redox homeostasis **(figure 3.1C)**. Introducing pyruvate or alpha ketobutyrate provides substrate to allow for the restoration of NAD+/NADH, possibly due to the cell's ability to carry on with glycolysis, and decreases complex 1 expression, restoring it to levels comparable to those seen under high glucose conditions.

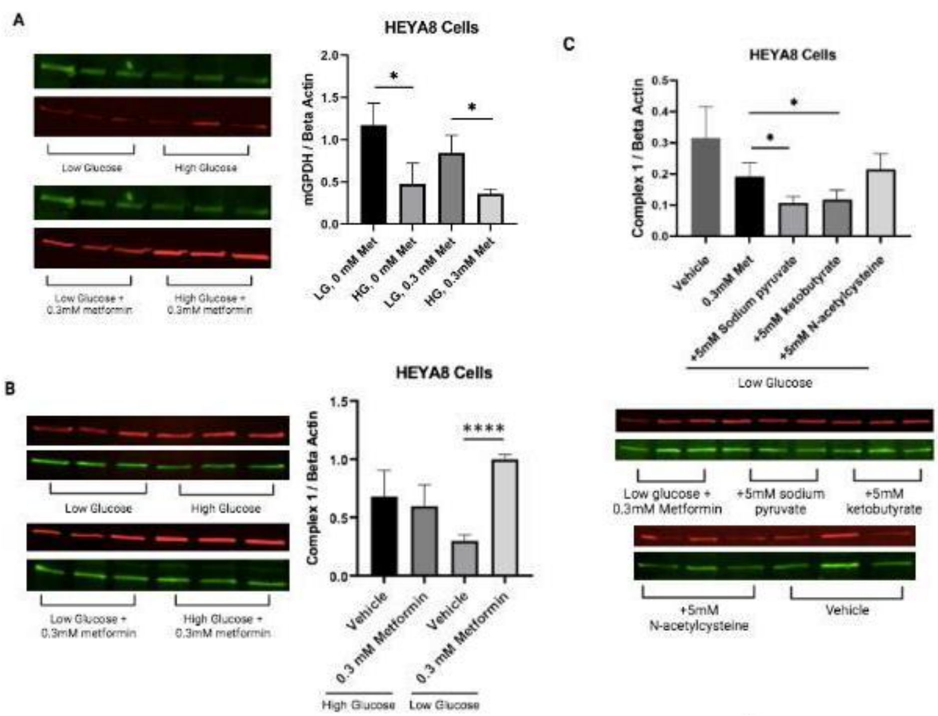

Figure 3.1. Analysis of protein levels in HEYA8 cells. mGPDH expression (green) relative to beta actin (A) after treatment with 5nM rotenone, 40uM metformin, and 200uM metformin. Complex 1 expression (green) relative to beta actin (B). Analysis of relative complex 1 protein expression under low glucose conditions and treated with sodium pyruvate, ketobutyrate, and N-acetylcysteine (C). Complex 1 levels were measured by probing the NDUFAF1 *p<0.05, **p<0.01, ***p<0.0001. Data are mean ± SD.

Next, we evaluated protein expression in C2C12 proliferating myocytes after metformin treatment and showed that mGPDH both mGPDH and Complex 1 are overexpressed compared to the controls **(figure 3.2A-B)**. We were especially interested in complex 1 being overexpressed since metformin is reported to be a complex 1 inhibitor. We believe that proliferating cells are able to compensate for weak inhibition due metformin and overexpress complex 1 to avoid cell death. Furthermore, we did not report any significant changes to AMPK phosphorylation due to low doses of metformin treatment, while the strong complex 1 inhibitor rotenone causes significant AMPK phosphorylation **(figure 3.2C).** These results confirm that previous studies using supra-pharmacological concentrations of metformin that show AMPK activation may be reporting that metformin has a significantly stronger effect on cells than actually seen *in vivo*.

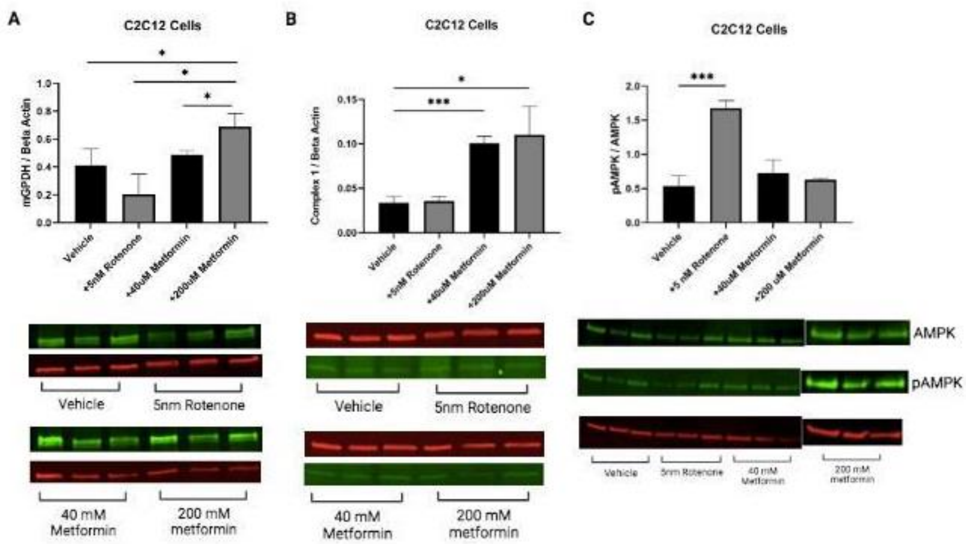

Figure 3.2. Analysis of protein levels in C2C12 myocytes. mGPDH expression (green) relative to beta actin (A) after treatment with 5nM rotenone, 40uM metformin, and 200uM metformin. Complex 1 expression (green) relative to beta actin (B). pAMPK/AMPK ratio expressed (green) relative to beta actin (C) *p<0.05, **p<0.01, ***p<0.0001. Data are mean ± SD.

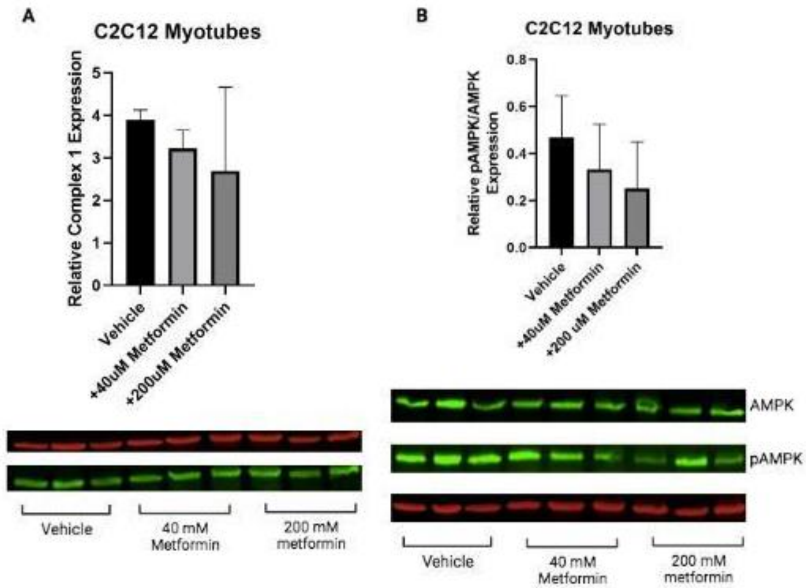

Figure 3.3. Analysis of protein levels in C2C12 differentiated myotubes. Complex 1 expression (green) relative to beta actin (A) after treatment with 5nM rotenone, 40uM metformin, and 200uM metformin. pAMPK/AMPK ratio expressed (green) relative to beta actin (B). *p<0.05, **p<0.01, ***p<0.0001. Data are mean ± SD.

We then proceeded to evaluate the effect of metformin on non proliferating, C2C12 differentiated myotubes. These cells are known to have increased rates of metabolism and a higher mitochondrial density, therefore we predicted that metformin would have different effects on these cells considering metformin's effect on mitochondrial metabolism. Unlike the myocytes, C2C12 myotubes did not show increased expression of complex 1 after metformin treatment, and like in the myocytes, there were no effects on pAMPK/AMPK ratios **(figure 3.3)**. There were also no significant changes in NAD+/NADH ratios **(figure 3.4A)**, AMP/ATP ratios **(figure 3.4B)**, and no alterations in glucose consumption or lactate production indicating no changes in the rate of glycolysis **(figure 3.4C)**. The lack of significant alterations in flux through glycolysis is consistent with the fact that we fail to see any sign of AMPK activation, indicating that metformin's mechanisms are AMPK independent.

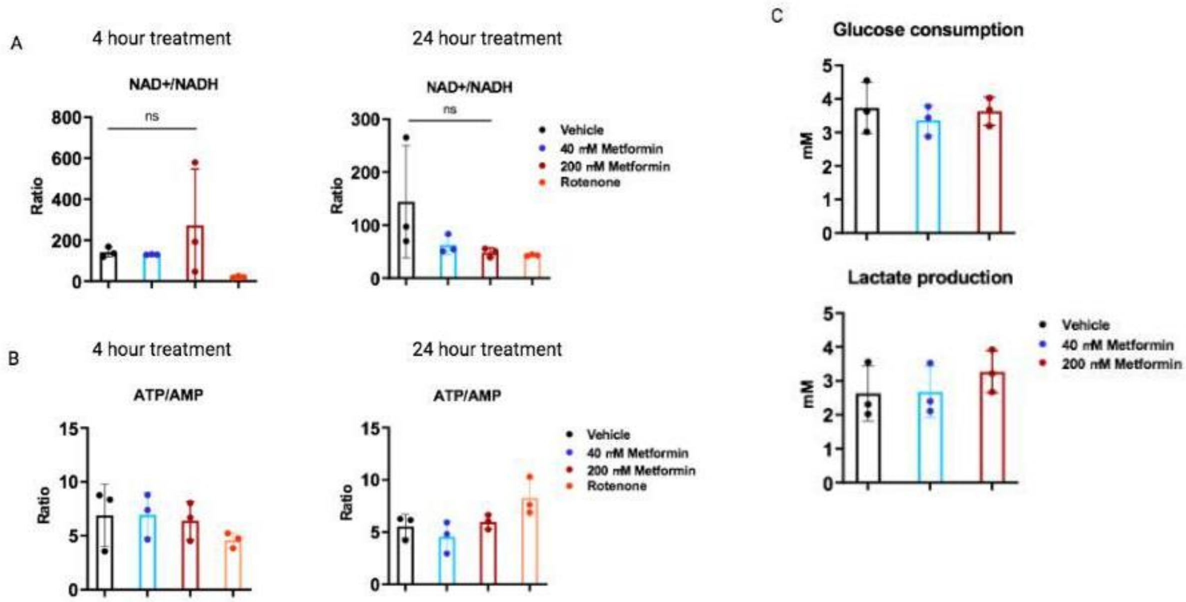

Figure 3.4. LCMS analysis of redox, energy status in C2C12 myotubes, glucose consumption and lactate production. Ratio of NAD+/NADH detected after 4 hours and 24 hours of metformin treatment (A). Ratio of ATP/AMP detected after 4 hours and 24 hours of metformin treatment (B). Concentration of glucose consumption and lactate production after 4 hours of metformin treatment (C) $^*p<0.05$, $^{**}p<0.01$, $^{***}p<0.0001$. Data are mean ± SD.

Despite alterations in complex 1 and mGPHD expression in C2C12 mycoytes, cellular redox status seems to be unaltered based on LCMS analysis **(figure 3.5A)**. Treatment with the strong complex 1 inhibitor rotenone significantly oxidizes cellular redox status while metformin, a weak complex 1 inhibitor, seems to have no effect on total cellular redox status. Similarly, rotenone significantly diminishes C2C12 energy status, shown with lowered AMP/ATP ratios, while metformin has no significant effect **(figure 3.5B)**.

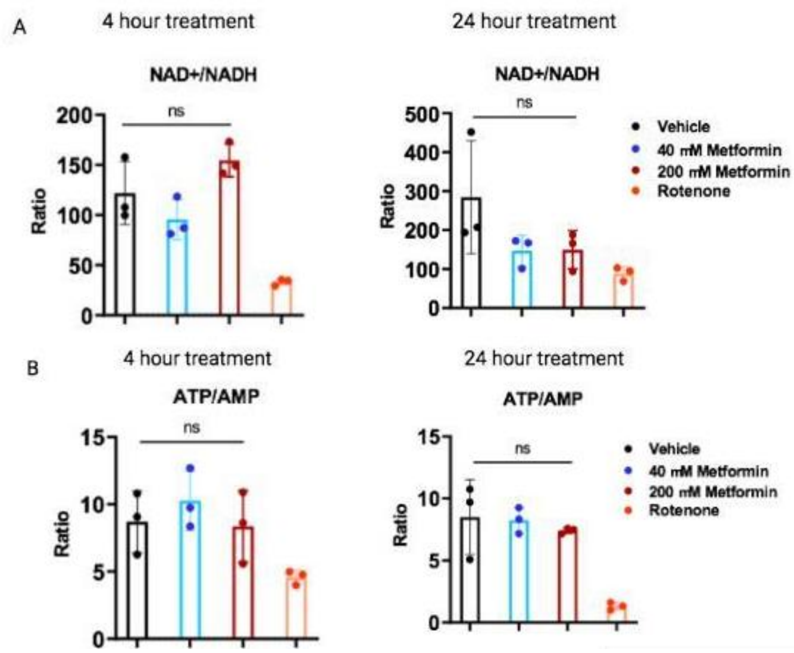

Figure 3.5. LCMS analysis of redox and energy status in C2C12 myocytes. Ratio of NAD+/NADH detected after 4 hour and 24 hour metformin treatment (A). Ratio of ATP/AMP detected after 24 hour metformin treatment (B). *p<0.05, **p<0.01, ***p<0.0001. Data are mean ± SD.

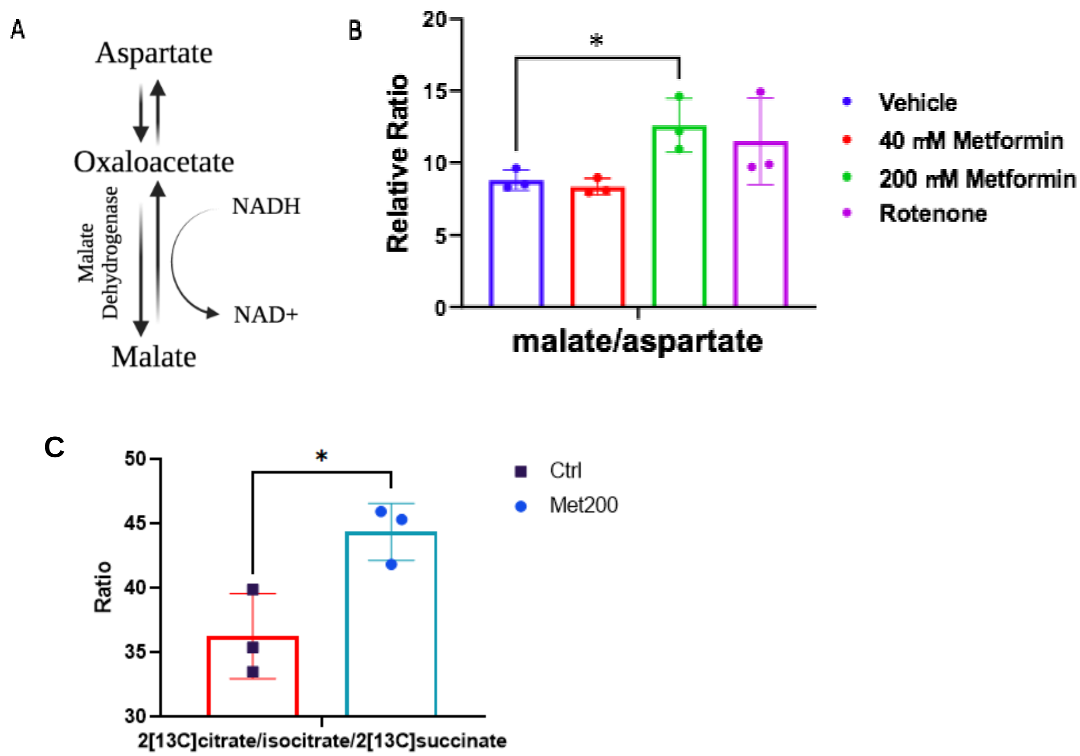

Figure 3.6. Analysis of redox status in C2C12 cells after metformin treatment. Scheme of aspartate to malate redox reaction (A). [M+2]Malate and [M+2]Aspartate ratios in C2Cl2 cells with [U-13C]-lactate treatment for 3 hours (B). Citrate (isocitrate) / succinate ratios after treatment with 200uM metformin. Values are expressed as mean ± SD of n=3 independent measurements. ns p>0.05, * p<0.05, ** p<0.01, *** p<0.001.

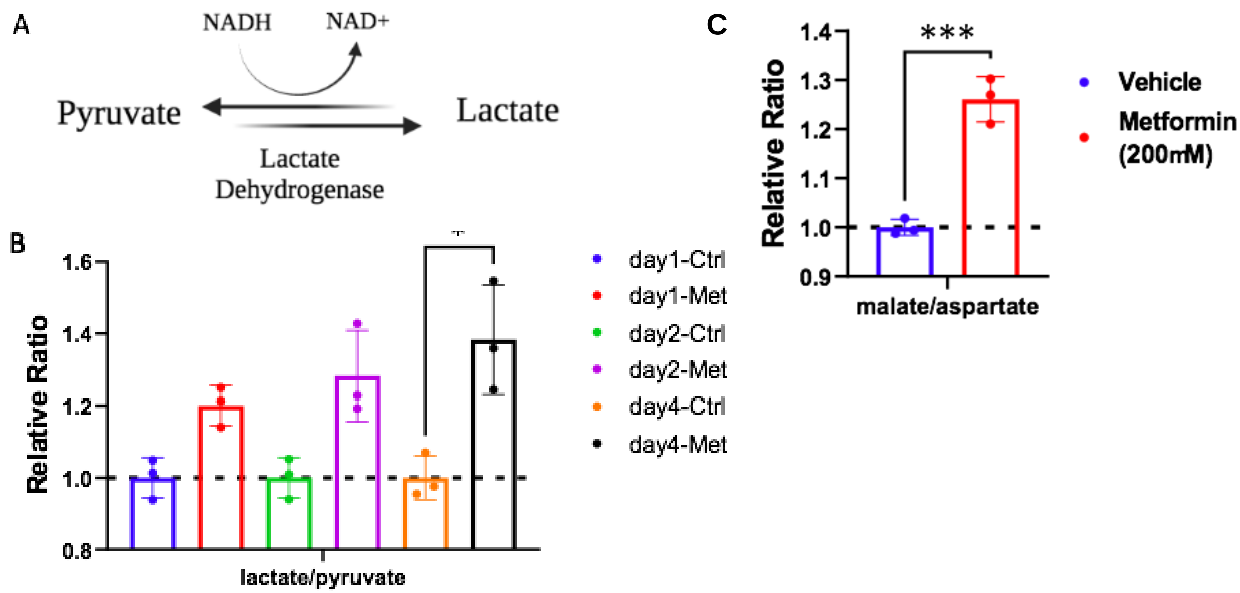

Figure 3.7. LCMS analysis of redox state in C2C12 myotubes. Scheme of pyruvate to lactate redox reaction (A). Lactate and pyruvate ratios in C2Cl2 cells at different treatment times (B). [M+2]Malate and [M+2]Aspartate ratios in C2Cl2 cells with [U-13C]-lactate treatment for 3 hours (C). Values are expressed as mean ± SD of n=3 independent measurements. ns p>0.05, * p<0.05, ** p<0.01, *** p<0.001.

Interestingly, despite having no detectable effects on NAD+/NADH ratios, metformin treatment both long term and short term, has the ability to increase lactate/pyruvate, malate/aspartate, and citrate/succinate ratios **(figure 3.6-3.7)**. While free pool NAD+/NADH remained unchanged, redox dependent mitochondrial reactions were altered by metformin treatment, further indicating that metformin does indeed target mitochondrial metabolism and acts in a redox dependent manner. We also conducted proteomics analysis on C2C12 myocytes and noticed a slight, but significant decrease in lactate dehydrogenase (LDH) expression, specifically lactate dehydrogenase B chain (LDHB) **(figure 3.8 B-C)**.

Figure 3.8. Proteomics analysis of C2C12 cells treated with metformin. A volcano plot showing proteomic analysis data after 40uM (A) and200uM (B) of metformin treatment, and 5nM of rotenone (C) Labeled are acyl-coA dehydrogenase and lactate dehydrogenase chain B. Significance is based on log(2) fold change of greater than 1 or less than -1 and a -10log P value greater than 1.35.

A

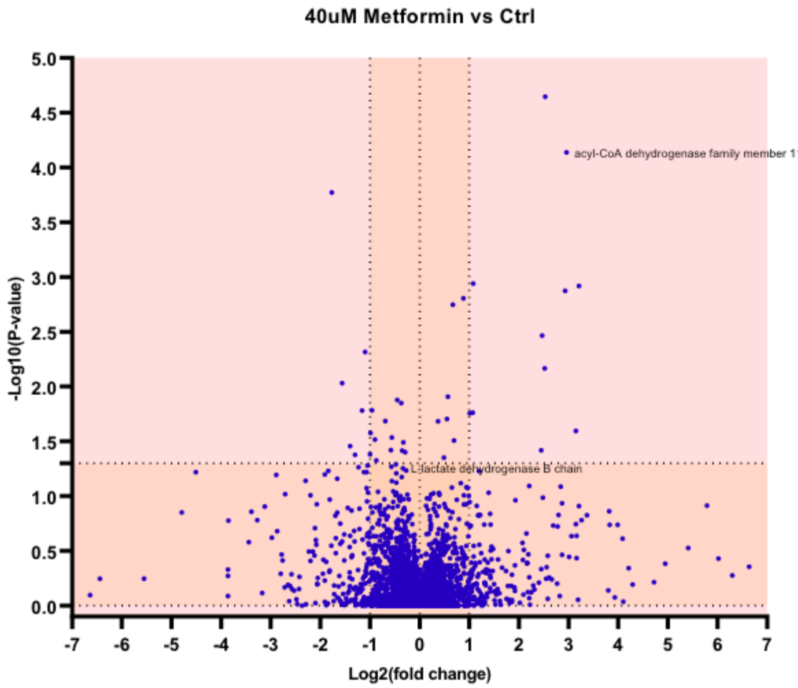
40uM Metformin vs Ctrl
acyl-CoA dehydrogenase family member 11
L-lactate dehydrogenase B chain
-Log10(P-value)
Log2(fold change)

B

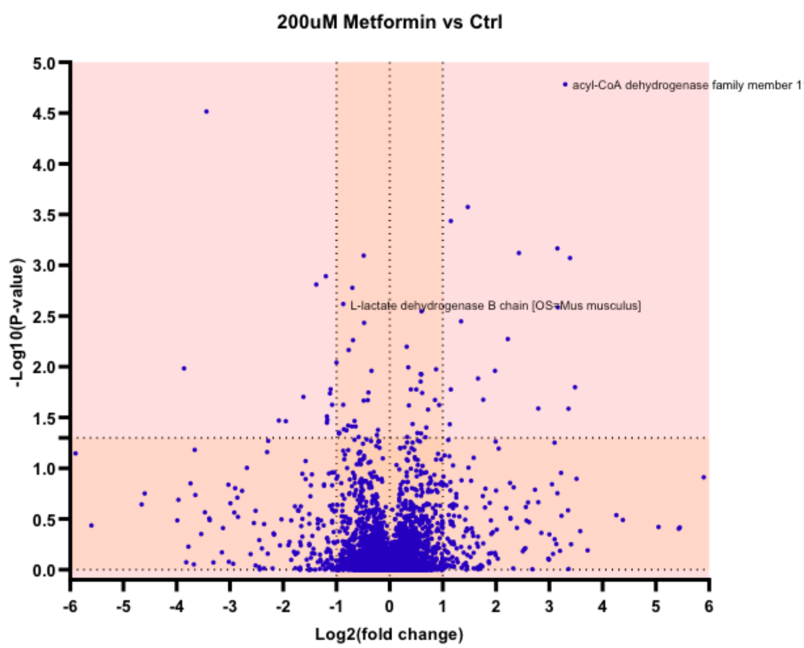
200uM Metformin vs Ctrl
acyl-CoA dehydrogenase family member 11
L-lactate dehydrogenase B chain [OS=Mus musculus]
-Log10(P-value)
Log2(fold change)

C

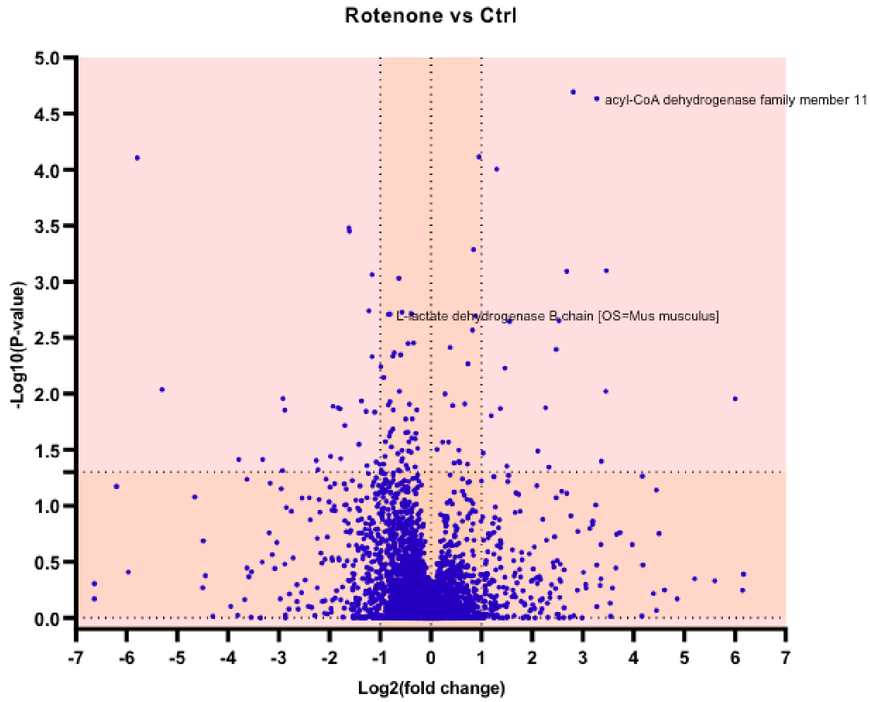

Our proteomics results also indicated that metformin, as well as rotenone, results in significant overexpression of proteins in the acyl-CoA dehydrogenase family, which catalyze the first step of each fatty acid beta-oxidation cycle in the mitochondria **(figure 3.8A-C)**. Overexpression of enzymes in this protein family is a strong indicator that metformin causes an increase in fatty acid catabolism.

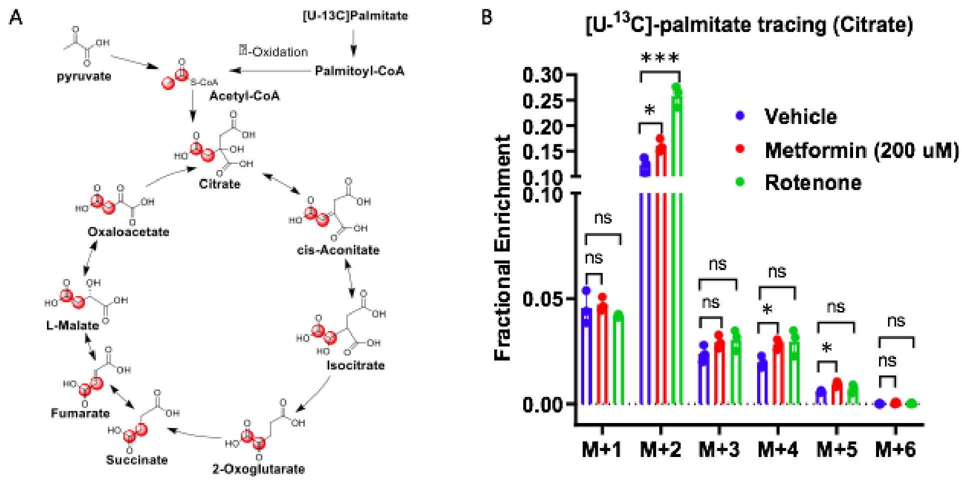

Figure 3.9. [U-13C] Palmitate tracing shows an increase in citrate production after metformin treatment. Schematic showing the molecular pathway of 13C labeled palmitate through beta-oxidation and Krebbs cycle (A) 13C tracing analysis using a tracer [U-13C]-palmitate for measuring fatty acid oxidation in C2C12 myotubes with different treatments for 2 days (B). Values are expressed as mean ± SD of n=3 independent measurements. ns p>0.05, * p<0.05, ** p<0.01, *** p<0.001.

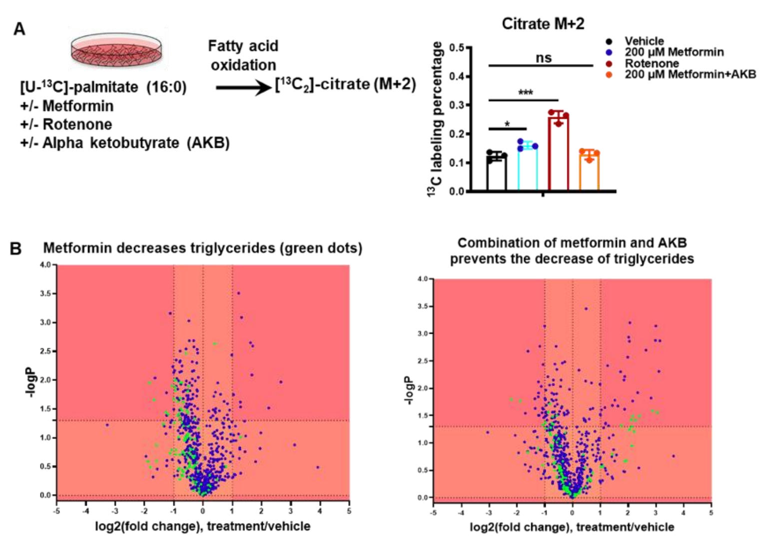

Figure 3.10. The effects of alpha-ketobutyrate on fatty acid oxidation and triglycerides in C2C12 cells. 13C tracing analysis using a tracer [U-13C]-palmitate for measuring fatty acid oxidation in C2C12 cells with different treatments for 2 days (A)**.** Volcano plots of detected lipids showing lipidomic alterations by metformin or the combination with alpha ketobutyrate (AKB) treatment in C2C12 cells for 4 days (B). Triglycerides are highlighted as green dots. Fold change and p values were calculated based on the relative intensity was calculated based on individual lipid peak area values in LC-MS data using a two-tailed unpaired Student's t test. Values are expressed as mean ± SD of n=3 independent measurements. ns p>0.05, * p<0.05, ** p<0.01, *** p<0.001.

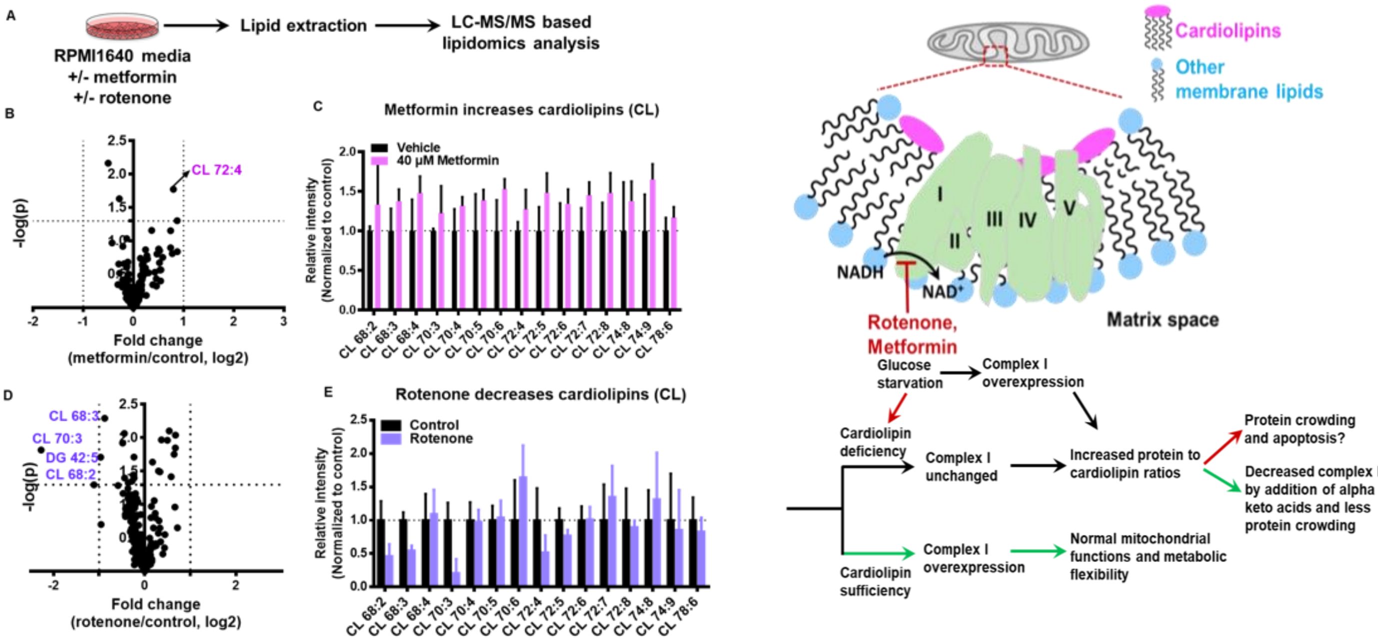

Figure 3.11. The effect of metformin and rotenone on fatty acid oxidation in C2C12 cells. A schematic illustration of lipidomics analysis workflow (A) Volcano plots of lipid alterations by metformin (B) and rotenone (D); Bar plots of representative cardiolipins after metformin treatment (C) and rotenone treatment (E). A schematic showing proposed relationship between complex 1 inhibition and cardiolipins (F) The relative intensity was calculated based on individual lipid peak area values in LC-MS data. Abbreviations: CL, Cardiolipin; DG,Diacylglycerol; CE, Cholesterol ester.

Although complex 1 has been studied time and time again as an important regulator of cellular redox state, its role in modulating lipid homeostasis and metabolism is not well understood. We show that complex 1 slightly increases the rate of fatty acid oxidation, as seen by 13C palmitate tracing. The strong complex 1 inhibitor rotenone increases flux through beta oxidation to a greater extent than metformin does, as indicated by increased citrate levels **(figure 3.9B)**. Despite no effect seen on redox status when directly measuring free pool NAD+, NADH, and NAD+/NADH ratios, changes in lactate/pyruvate, malate/aspartate, citrate/succinate ratios, and decreased LDHB expression indicate otherwise. Additionally, cells treated with metformin in addition to alpha-ketobutyrate, and saw that the metformin induced increase in fatty acid oxidation **(figure 3.10A)** and metformin induced decrease in triglyceride stores **(figure 3.10B)** were reversed to levels seen without metformin treatment, indicating that metformin’s mechanisms of action are likely redox dependent.

We have shown that metformin triggers a cellular adaptive response in which treated cells overexpress complex 1, which is the largest protein subcomplex of the mitochondrial membrane. Cardiolipins are known to bind tightly to proteins, so we analyzed the effect of metformin on cardiolipin levels **(figure 3.11)**. We found that metformin induced an increase in cardiolipin levels while rotenone resulted in a decrease in cardiolipin levels **(figure 3.11B-E).** Our data suggests that metformin induced stress triggers an adaptive response which induces complex 1 overexpression and a corresponding increase in cardiolipin levels, increased flux through metabolism, and decreased triglyceride stores.

3.4. Discussion

As shown in previous figures, reliably capturing alterations in redox state is difficult due to the simple fact that there are a plethora of redox reactions constantly happening at any given point in time, and quantification of cellular NAD+/NADH may not capture subtle changes that a weak inhibitor such as metformin seems to have. Cells also have natural buffer systems in which certain redox reactions will compensate for the underproduction, or overproduction of NAD+ or NADH. In this case, the increased ratios of lactate/pyruvate, malate/aspartate, and citrate/succinate indicate high NADH/NAD+ levels within the mitochondria, which we propose is due to metformin induced complex 1 inhibition. To support this, our proteomics analysis showed decreased expression of LDHB, which has an affinity for lactate and NAD+, rather than pyruvate and NADH. Therefore, LDHB under expression in cells treated with 200uM metformin and 5nM rotenone, suggest that metformin, like rotenone, inhibits complex 1 and increases mitochondrial NADH/NAD+, and subsequently inhibits LDHB expression.

HEYA8 ovarian cancer cells and C2C12 myocytes both show evidence of complex 1 overexpression, which we propose is an adaptive response promoted by weak complex 1 inhibition triggered by treatment with pharmacologically relevant doses of metformin. Previous studies show that millimolar concentrations are required to inhibit isolate complex 1 while micromolar levels are able to do so in intact cells, [6] which we confirm with our data. This suggests that metformin may either trigger a signaling pathway, which is yet to be mapped out, or metformin accumulates within the mitochondria until there is a high enough concentration to inhibit complex 1. Our imaging studies from Chapter 2 show that, in certain cells, there may be accumulation of metformin within the mitochondria.

We also note alterations in lipid metabolism, and cardiolipin levels, which may be tied to metformin induced changes to complex 1 levels or may be directly affected by metformin. In C2C12 myotubes, we note similar alterations in lipid metabolism but no detectable changes in complex 1 protein levels. This may best be explained by the cells' ability to better adapt to complex 1 inhibition due to their higher metabolic activity and higher mitochondrial density. Compensating for complex 1 inhibition by overexpressing the enzyme is an energy-consuming anabolic process and since these cells have high metabolic activity, they may be able to mediate cell induced stress by decreasing NAD+ consuming reactions and increasing NAD+ producing reactions.

Complex 1 activity and assembly of respiratory chain complexes are closely tied to fatty acid oxidation membrane lipid remodeling,[13,14,15] such as the content and acyl chain compositions of cardiolipins and phosphatidylethanolamine (PE). It has been shown that cardiolipin composition on inner mitochondrial membrane is very dynamic, and responsive to various factors, such as fatty acyl environment[16] , increased metabolic demand[17] , and cell cycle.[18] We show that the strong complex 1 inhibitor rotenone decreases cardiolipin levels within the cell while the weak inhibitor metformin, which according to our western blot data results in a compensatory overexpression of complex 1, results in higher levels of cardiolipins which are important components of the inner mitochondrial membrane. These results suggest that metformin increases cellular cardiolipin requirements in order to combat the mitochondrial stress inflicted by metformin treatment.

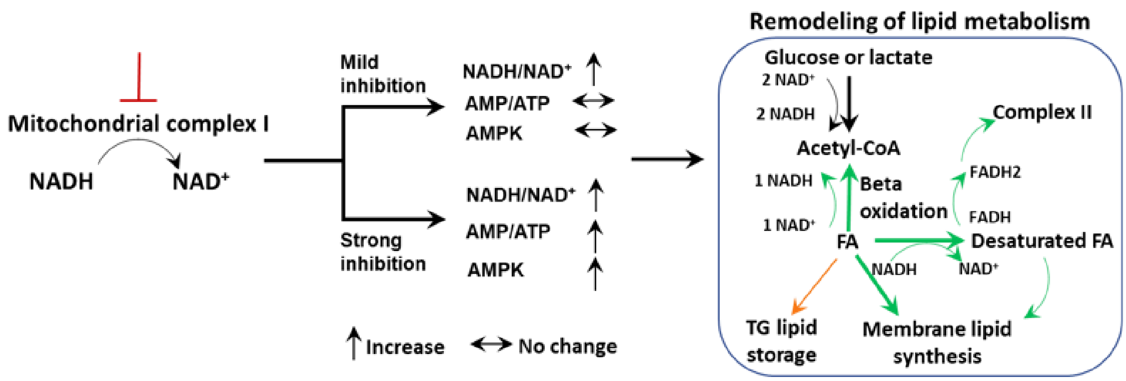

Figure 3.12. Proposed model illustrating remodeling of lipid metabolism in response to complex I inhibition. Arrows denote a potential increase (green arrow) or decrease (yellow arrow) by complex I inhibition. FA, fatty acid; TG, triglycerides; AMPK, AMP-activated protein kinase.

Even though complex 1 has long been studied as an important redox and energy regulator within the cell and has been shown to promote fatty acid oxidation and lower triglyceride storage levels, it has been thought to do so through AMPK activation. However, we found that weak inhibition of complex 1 does not alter AMPK activation levels and may not be the mechanism through which metformin alters lipid metabolism **(figure 3.14)**. There may be a few reasons why cells increase fatty acid oxidation; complex 1 inhibition increases NADH/NAD+ ratios and glucose metabolism requires 2 NAD+ per acetyl-CoA produced while beta oxidation only requires one and/or fatty acid oxidation produces FADH2 which can be fed to complex II, essentially bypassing complex 1 and compensating for its inhibition. Fatty acid oxidation also provides substrate for membrane lipid synthesis, which may be necessary to allow for mitochondrial adaptation to metformin induced stress.

Our studies provide evidence that metformin does indeed target the mitochondria, is a weak complex 1 inhibitor (which allows the mitochondria to alter protein expression and metabolism to adapt so this stress), and alters lipid metabolism through and AMPK independent molecular mechanism. Our data provides key information that helps piece together the puzzle that is metformin's mechanism of action, especially because we carry out our experiments using pharmacologically relevant doses of metformin in various cell types.

3.5. Materials and Methods

Table 2. Chapter 3 materials list. List of materials used to conduct experiments for Chapter 3

Antibodies	Product	Source	Identifier
	2-propanol	Fisher Chemical	A461-4
	AMPKα (D5A2) Rabbit mAb	Cell Signaling Technology	#5831T
	β-Actin (8H10D10) Mouse mAb	Cell Signaling Technology	8H10D10
	Ethyl Acetate	Supelco	CAS-No. 141-78-6
	Goat anti-Mouse IgG DyLight ™ 650	ThermoFisher Scientific	84545
	Goat anti-Rabbit IgG Alexa Fluor ™ Plus 800	Invitrogen	A32735
	GPD2 Polyclonal antibody	proteintech	Cat# 17219-1AP
	NDUFAF1 Polyclonal antibody (Complex 1)	proteintech	15181-1-AP
	NDUFS1 Polyclonal antibody (Complex 1)	Proteintech	12444-1-AP
	Phospho-AMPKα (Thr172) (40H9) Rabbit mAb	Cell Signaling Technology	#2535T

Table 2 (continued)

Commercial Assays	Product	Source	Identifier
	Pierce™ BCA Protein Assay Kit	ThermoFisher Scientific	REF 23225

Instruments	Product	Source	Identifier
	CentriVap ® Centrifugal Concentrator and Cold Trap	Labconco	NA
	Mini-PROTEAN® Tetra System	BIO-RAD	165-8004
	Odyssey CLx	LI-COR	NA

Reagent or Resource	Product	Source	Identifier
	10x Tris/Glycine (TG) Buffer	BIO-RAD	Cat. #161-0771
	10x Tris/Glycine/SDS (TGS) Buffer	BIO-RAD	Cat. #1610772
	2-Mercaptoethanol (BME)	VWR	M131-100ML
	4X Lamli Buffer	BIO-RAD	Cat. # 161-0747
	Albumin, Bovine (BSA)	VWR	0332-25G
	Ammonium Bicarbonate (ABC)	Fisher	A643-500
	Chameleon® Duo Pre-stained Protein Ladder	LI-COR	P/N: 928-60000
	Hydrochloric acid	VWR	BDH7419-1
	Immun-Blot® PVDF Membranes for Protein Binding	BIO-RAD	Cat: #1620177
	LC Vial Caps	Waters Corp.	WAT094174

Table 2 (continued)

	LC Vials	Waters Corp.	WAT094172
	Lipid Standards	Dr. Wei-chen Chang's Lab at NCSU	NA
	Magnesium Chloride (MgCl2)	Beantown Chemical	214515-1KG
	Methanol (Suitable for UHPLC-UV)	Fisher	A412-4
	Mini-Protean® TGX Stain-Free™ Precast Gel (4-20%)	BIO-RAD	CAT. #456-8094
	Pierce™ Protease and Phosphatase Inhibitor	ThermoFisher Scientific	Prod# A32961
	Pierce™ RIPA Buffer	ThermoFisher Scientific	89900
	Potassium Chloride (KCl)	MP Bio	Cat No. 151944
	Rotenone	Cayman Chemical	Item no. 13995
	Sodium deoxycholate (SDC)	Alfa Aesar	J62288
	Sodium 2-oxobutyrate	Sigma Aldrich	K0875-5G
	Sodium Azide 5% w/v	VWR	BDH7465-2
	Sodium Chloride (NaCl)	Macron	7532-06
	Sodium deoxycholate	Alfa Aesar	J62288-14
	Sodium hydroxide	VWR	BDH7247
	Sodium Pyruvate (C3H3NaO3)	Alfa Aesar	A11148
	Sucrose	VWR	M117-500G
	TRIS Hydrochloride (TrisCl)	VWE	M108-500G
	Trolox	EMD Millipore Corp	648471

Table 2 (continued)			
	Tween ® 20	VWR	M147-1L
	Water (Suitable for UHPLC-UV)	Fisher	W6-4

Software	Product	Source	Identifier
	Graphpad Prism		NA
	Image Studio Version 5.x	LI-COR	NA
	Sieve		NA

Cell Culture

All cells were cultured in 10 cm dishes with full growth medium containing RPMI 1640, 10% FBS, and 1% penicillin-streptomycin. All cells were incubated at 37ºC and 5% CO2. Cells were split at 75% - 85% confluence at a 1:20 ratio and were discarded past the recommended number of passages. C2C12 cells were provided by the Tissue Culture Facility (TCF) at UNC Lineberger. HEYA8 OvCa cells were donated by Dr. Ernst Lengyel's lab at the University of Chicago.

Protein Extraction

Proteins were extracted one of two ways: using RIPA buffer or using an MTBE-methanol extraction protocol suitable for LC-MS analysis.

Ripa Buffer Protein Extraction

Cell medium was first aspirated and cells were gently rinsed twice with ice cold PBS. 500 uL of PBS was added to each well and cells were scraped into the solution and collected in microcentrifuge tubes. Cells were then pelleted by spinning down at 2500x g for 5 minutes. The PBS was aspirated, leaving the pellet in the tube, and 100uL of RIPA buffer with protease and phosphatase inhibitor. We used Pierce™ Protease and Phosphatase Inhibitor and followed the manufacturer's protocol. After the addition of RIPA buffer and protease inhibitor, samples were vortexed for 1 minute then rocked on ice for 15 minutes and centrifuged at 14000x g for 15 minutes at 4ºC. The supernatant was collected into a new tube and further analyses were conducted.

Metabolite and Protein Extraction for LC-MS

Polar metabolites, nonpolar metabolites and proteins extracted for analysis by LC-MS were extracted using an MTBE-methanol extraction method. Cells plated in 6-well plates were first rinsed with ice cold 0.9% NaCl and immediately placed on dry ice to minimize continued cellular activity. Pre-cooled 80% methanol was added to each well, and left in the -80ºC freezer for 15 minutes before being scraped off and transferred into individual 15mL centrifuge tubes. Once transferred to the tube, samples were vortexed for one minute, 2.4 mL of ice cold HPLC grade MTBE was added, and samples were vortexed again for one minute. Internal standards were then added (5uL of lipid standards and 10uL of e-coli extract). We then added 0.6mL ice cold HPLC grade water to each tube and vortexed for one minute, resulting in a final ratio of 1 part MeOH, 3 parts MTBE, and 1 part H2O by volume. Samples were then centrifuged at 4000 xg for 10 minutes at 4ºC during which the solvent layers separated. The top layer contained the MTBE and lipid metabolites, the bottom layer contained the H2O and the polar metabolites, and the proteins were pelleted at the bottom of the tube. Each layer was separated into microcentrifuge tubes making sure to avoid contamination from the other layer by discarding any solute where the two layers met. The lipid and polar samples were dried in a speed vacuum at room temperature and stored at -80ºC until they were ready to be analyzed. Protein pellets were left to dry at room temperature and then resuspended in an ABC/SDC buffer with 50mM ABC (ammonium bicarbonate), 1% sodium deoxycholate and 2.5mM pyruvate.

Protein Concentration Determination

To determine protein concentration of extracted proteins we used a BCA protein assay in a 96 well plate. Each well contained either 5uL of sample or 5uL of standard. Wells with standard also had 5uL saline solution and wells with standard had either 5uL ABC/SDC buffer or 5uL Ripa buffer with protease inhibitor depending on protein extraction method. Standard concentrations were the following: 2 ug/ul, 1.5 ug/ul, 1 ug/ul, 0.75 ug/ul, 0.5 ug/ul, 0.25 ug/ul, 0.125 ug/ul, 0.025 ug/ul, and 0 ug/ul. 200 uL of BCA reagent (Reagent A: Reagent B, 50:1, v/v) was added to each well. The plate was incubated at 37ºC for 30 minutes and read at 562 nm absorbance using BioTek's Cytation 5 Imaging Reader. After BCA analysis, samples were normalized so that each contained 0.5-1.0 ug of protein per uL.

Western Blot Analysis

Samples were diluted to have 10ug of total protein at the time of loading. Proteins from each sample were mixed with 25% volume of 4x Laemmli sample buffer which included 10% 2-mercaptoethanol (BME). Samples were loaded into the 4-20% Mini-Protean® TGX Stain-Free Gels at 20uL per well resulting in total protein concentrations of 10-20ug unless otherwise stated, and 7uL of Chameleon® Duo Pre-stained Protein Ladder. The inner chamber of the system was filled with 200mL of 1x TGS running buffer (10x Tris/Glycine/SDS:water, 1:9, v/v). The gels were run briefly at 120 V and then increased to 200 V using the BIO-RAD Mini-PROTEAN® Tetra System. Gels were run until desired separation was acquired. After gel electrophoresis, proteins were transferred onto Immun-Blot® PVDF Membranes using a cold, wet transfer method at 300mA for 35 minutes for one gel and 45 minutes for 2 gels. The system was filled with 400mL TG transfer buffer (Tris/Glycine:water:methanol, 1:7:2, v/v/v). Once the protein transfer was completed, membranes were blocked in 5% non-fat milk made up in TBST buffer (10x TBS:water, 1:9, v/v) with 0.05% Tween®. 10x TBS buffer was made using 15.76g TrisCl, 43.83g NaCl, and 500 mL Water. NaOH or HCl were added one drop at a time until a pH of 7.2-7.4 was achieved. Once blocked, membranes were probed for the desired proteins. Membranes were incubated with primary antibodies at a 1:1000 ratio overnight at 4ºC, washed three times, incubated with secondary antibodies at a 1:5000 ratio for one hour at room temperature, washed three times, then imaged using LI-COR's Odyssey CLx. When necessary, PVDF membranes were stripped using a harsh stripping buffer to allow for reprobing of similarly sized proteins. Harsh stripping buffer was made using 6% Tris pH 6.8, 0.7% BME, 10% of a 20% SDS solution, and 83.3% deionized water.

HPLC method. The analysis of metabolites in mouse tissues and plasma was performed using Ultimate 3000 UHPLC (Dionex), while the analysis of metabolites from cultured cells was performed using Vanquish UHPLC (Thermo Fisher Scientific). A hydrophilic interaction chromatography method (HILIC) with an Xbridge amide column (100 x 2.1 mm i.d., 3.5 m; Waters) was used for compound separation at 25 °C. Mobile phase A: water with 5 mM ammonium acetate (pH 6.8), and mobile phase B: 100 % acetonitrile. Linear gradient is: 0 min, 85% B; 1.5 min, 85% B; 5.5 min, 35% B; 6.9 min, 35% B; 10.5 min, 35% B; 10.6 min, 10% B; 12.5 min, 10% B; 13.5 min, 85% B; 17.9 min, 85% B; 18 min, 85% B; 20 min, 85% B. Due to the instrumentation difference between Ultimate 3000 UHPLC and Vanquish UHPLC, different flow rates were used. For Ultimate 3000 UHPLC, the flow rate is: 0-5.5 min, 0.15 ml/min; 6.9-10.5 min, 0.17 ml/min; 10.6-17.9 min, 0.3 ml/min; 18-20 min, 0.15 ml/min. For Vanquish

UHPLC, the flow rate is: 0-5.5 min, 0.11 ml/min; 6.9-10.5 min, 0.13 ml/min; 10.6-17.9 min, 0.25 ml/min; 18-20 min, 0.11 ml/min.

Mass Spectrometry

The analysis of metabolites in mouse tissues and plasma was performed using Q Exactive Plus mass spectrometer (Thermo Fisher Scientific), while the analysis of metabolites from cultured cells was performed using Orbitrap Exploris 480 mass spectrometer (Thermo Fisher Scientific). Both mass spectrometers are equipped with a HESI probe and operated in the positive/negative switching mode. When Q Exactive Plus mass spectrometer was used, the relevant parameters are as listed: heater temperature, 120 °C; sheath gas, 30; auxiliary gas, 10; sweep gas, 3; spray voltage, 3.6 kV for positive mode and 2.5 kV for negative mode; capillary temperature, 320°C; S-lens, 55. The resolution was set at 70,000 (at *m/z* 200). Maximum injection time (max IT) was set at 200 ms and automated gain control (AGC) was set at 3×10^6. When Exploris 480 mass spectrometer was used, the relevant parameters are as listed: vaporizer temperature, 350 °C; ion transfer tube temperature, 300 °C; sheath gas, 35; auxiliary gas, 7; sweep gas, 1; spray voltage, 3.5 kV for positive mode and 2.5 kV for negative mode; RF-lens (%), 30. The resolution was set at 60,000 (at *m/z* 200). Automatic maximum injection time (max IT) and automated gain control (AGC) were used.

Data analysis and statistics

LC-MS peak extraction and integration were performed using commercially available software Sieve 2.0 (Thermo Fisher Scientific). The integrated peak area was used to calculate ^{13}C enrichment. Natural abundance correction was performed using software R with Bioconductor R package IsocorrectionR [32]. All data are represented as mean ± SD. All p values are obtained from the student's t-test two-tailed using GraphPad Prism 8 unless otherwise noted.

References

1. Liu, X.; Romero, I. L.; Litchfield, L. M.; Lengyel, E.; Locasale, J. W. Metformin Targets Central Carbon Metabolism and Reveals Mitochondrial Requirements in Human Cancers. Cell Metabolism 2016, 24 (5), 728–739. https://doi.org/10.1016/j.cmet.2016.09.005.

2. Owen, M. R.; Doran, E.; Halestrap, A. P. Evidence That Metformin Exerts Its Anti-Diabetic Effects through Inhibition of Complex 1 of the Mitochondrial Respiratory Chain. 2000, 8.

3. Pernicova, I.; Korbonits, M. Metformin—Mode of Action and Clinical Implications for Diabetes and Cancer. Nat Rev Endocrinol 2014, 10 (3), 143–156. https://doi.org/10.1038/nrendo.2013.256.

4. Madiraju, A. K.; Qiu, Y.; Perry, R. J.; Rahimi, Y.; Zhang, X.-M.; Zhang, D.; Camporez, J.-P. G.; Cline, G. W.; Butrico, G. M.; Kemp, B. E.; Casals, G.; Steinberg, G. R.; Vatner, D. F.; Petersen, K. F.; Shulman, G. I. Metformin Inhibits Gluconeogenesis via a Redox-Dependent Mechanism in Vivo. Nat Med 2018, 24 (9), 1384–1394. https://doi.org/10.1038/s41591-018-0125-4.

5. Wheaton, W. W.; Weinberg, S. E.; Hamanaka, R. B.; Soberanes, S.; Sullivan, L. B.; Anso, E.; Glasauer, A.; Dufour, E.; Mutlu, G. M.; Budigner, G. S.; Chandel, N. S. Metformin Inhibits Mitochondrial Complex I of Cancer Cells to Reduce Tumorigenesis. eLife 2014, 3, e02242. https://doi.org/10.7554/eLife.02242.

6. Fontaine, E. Metformin-Induced Mitochondrial Complex I Inhibition: Facts, Uncertainties, and Consequences. Front. Endocrinol. 2018, 9, 753. https://doi.org/10.3389/fendo.2018.00753.

7. Pecinová, A., Brázdová, A., Drahota, Z., Houštěk, J., & Mráček, T. (2019). Mitochondrial targets of metformin—are they physiologically relevant? BioFactors, 45(5), 703–711. https://doi.org/10.1002/biof.1548

8. MacDonald, M. J.; Ansari, I. H.; Longacre, M. J.; Stoker, S. W. If Metformin Inhibited the Mitochondrial Glycerol Phosphate Dehydrogenase It Might Not Benefit Diabetes; preprint; Biochemistry, 2020.

9. Thakur, S.; Daley, B.; Gaskins, K.; Vasko, V. V.; Boufraqech, M.; Patel, D.; Sourbier, C.; Reece, J.; Cheng, S.-Y.; Kebebew, E.; Agarwal, S.; Klubo-Gwiezdzinska, J. Metformin Targets Mitochondrial Glycerophosphate Dehydrogenase to Control Rate of Oxidative Phosphorylation and Growth of Thyroid Cancer In Vitro and In Vivo. Clin Cancer Res 2018, 24 (16), 4030–4043. https://doi.org/10.1158/1078-0432.CCR-17-3167.

10. Zhou, G.; Myers, R.; Li, Y.; Chen, Y.; Shen, X.; Fenyk-Melody, J.; Wu, M.; Ventre, J.; Doebber, T.; Fujii, N.; Musi, N.; Hirshman, M. F.; Goodyear, L. J.; Moller, D. E. Role

of AMP-Activated Protein Kinase in Mechanism of Metformin Action. J. Clin. Invest. 2001, 108 (8), 1167–1174. https://doi.org/10.1172/JCI13505.

11. Wang, Y.; An, H.; Liu, T.; Qin, C.; Sesaki, H.; Guo, S.; Radovick, S.; Hussain, M.; Maheshwari, A.; Wondisford, F. E.; O'Rourke, B.; He, L. Metformin Improves Mitochondrial Respiratory Activity through Activation of AMPK. Cell Reports 2019, 29 (6), 1511-1523.e5. https://doi.org/10.1016/j.celrep.2019.09.070.

12. Zong, W.-X.; Rabinowitz, J. D.; White, E. Mitochondria and Cancer. Molecular Cell 2016, 61 (5), 667–676. https://doi.org/10.1016/j.molcel.2016.02.011.

13. Xu Y, Anjaneyulu M, Donelian A, Yu W, Greenberg ML, Ren M, Owusu-Ansah E and Schlame M. Assembly of the complexes of oxidative phosphorylation triggers the remodeling of cardiolipin. Proc Natl Acad Sci U S A. 2019;116:11235-11240.PMC6561273

14. Jussupow A, Di Luca A and Kaila VRI. How cardiolipin modulates the dynamics of respiratory complex I. Sci Adv. 2019;5:eaav1850.PMC6426460

15. Heden TD, Johnson JM, Ferrara PJ, Eshima H, Verkerke ARP, Wentzler EJ, Siripoksup P, Narowski TM, Coleman CB, Lin CT, Ryan TE, Reidy PT, de Castro Bras LE, Karner CM, Burant CF, Maschek JA, Cox JE, Mashek DG, Kardon G, Boudina S, Zeczycki TN, Rutter J, Shaikh SR, Vance JE, Drummond MJ, Neufer PD and Funai K. Mitochondrial PE potentiates respiratory enzymes to amplify skeletal muscle aerobic capacity. Sci Adv.

16. Oemer G, Edenhofer ML, Wohlfarter Y, Lackner K, Leman G, Koch J, Cardoso LHD, Lindner HH, Gnaiger E, Dubrac S, Zschocke J and Keller MA. Fatty acyl availability modulates cardiolipin composition and alters mitochondrial function in HeLa cells. J Lipid Res. 2021;62:100111.PMC8455370

17. Corrado M, Edwards-Hicks J, Villa M, Flachsmann LJ, Sanin DE, Jacobs M, Baixauli F, Stanczak M, Anderson E, Azuma M, Quintana A, Curtis JD, Clapes T, Grzes KM, Kabat AM, Kyle R, Patterson AE, Geltink RK, Amulic B, Steward CG, Strathdee D, Trompouki E, O'Sullivan D, Pearce EJ and Pearce EL. Dynamic Cardiolipin Synthesis Is Required for CD8(+) T Cell Immunity. Cell Metab. 2020;32:981-995 e7.PMC7721104

18. Chao YJ, Chang WH, Ting HC, Chao WT and Hsu YH. Cell cycle arrest and cell survival induce reverse trends of cardiolipin remodeling. PLoS One. 2014;9:e113680.PMC4244155

19. Kühlbrandt, W. Structure and Function of Mitochondrial Membrane Protein Complexes. BMC Biol 2015, 13 (1), 89. https://doi.org/10.1186/s12915-015-0201-x.

20. Sharma, L.; Lu, J.; Bai, Y. Mitochondrial Respiratory Complex I: Structure, Function and Implication in Human Diseases. CMC 2009, 16 (10), 1266–1277. https://doi.org/10.2174/092986709787846578.

21. Watmough, N. J.; Bindoff, L. A.; Birch-Machin, M. A.; Jackson, S.; Bartlett, K.; Ragan, C. I.; Poulton, J.; Gardiner, R. M.; Sherratt, H. S. A.; Tumbull, D. M. Impaired Mitochondrial A-Oxidation in a Patient with an Abnormality of the Respiratory Chain. 8.

22. Corsini GU, Sirigu F, Tagliamonte P and Muntoni S. Effects of biguanides on fatty acid and glucose oxidation in muscle. Pharmacol Res Commun. 1974;6:253-61

23. Gonzalez-Barroso MM, Anedda A, Gallardo-Vara E, Redondo-Horcajo M, Rodriguez-Sanchez L and Rial E. Fatty acids revert the inhibition of respiration caused by the antidiabetic drug metformin to facilitate their mitochondrial beta-oxidation. Biochim Biophys Acta. 2012;1817:1768-75